



中国科学技术大学

电子碰撞谱学的新机遇与新进展

陈向军



Hefei National Laboratory for Physical Science at Microscale
& Department of Modern Physics,
University of Science and Technology of China (USTC)





1. 背景
2. 电子与原子分子碰撞电离的实验和理论
 - (1) 实验技术
 - (2) 理论方法
3. $(e, 2e)$ 电子动量谱学的新进展
 - (1) 谱仪技术新进展;
 - (2) $(e, 2e)$ 的分子多中心干涉效应。
4. 扫描探针电子能谱学
 - (1) 谱仪技术的发展;
 - (2) 非线性非弹性电子散射现象。





1924，德布罗意提出了物质波假设

像电子这样的实物粒子也有波动性，称为物质波。

设一具有动能 T 、动量 p 和静止质量 m_0 的自由粒子，与它相联系的物质波的波长 λ 可以用光子的粒子性公式类比得到：

$$\lambda = \frac{h}{p} = \frac{h}{m_0 v} \sqrt{1 - \beta^2}$$

$$\lambda = \frac{hc}{\sqrt{E^2 - m_0^2 c^4}} = \frac{hc}{\sqrt{2m_0 c^2 T} \sqrt{1 + T / 2m_0 c^2}}$$

非相对论：

$$\lambda = \frac{h}{p} = \frac{h}{m_0 v} = \frac{h}{\sqrt{2m_0 T}}$$



Louis de Broglie
(1892-1987)

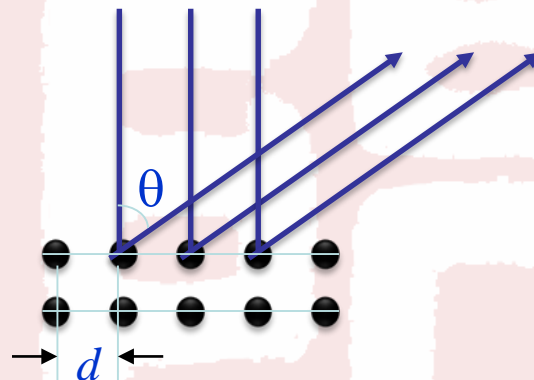
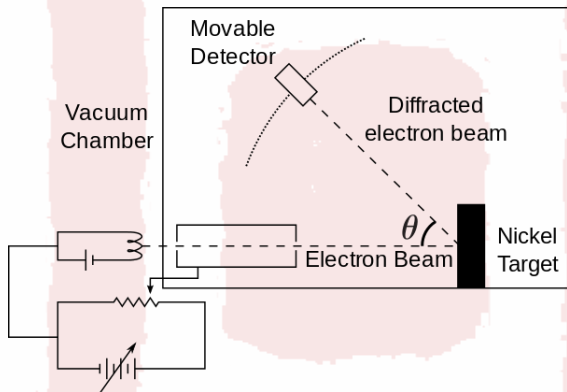
Einstein wrote shortly afterwards: "*I believe it is a first feeble ray of light on this worst of our physics enigmas*".



The Nobel Prize in Physics 1929



1927, 美国Bell实验室的戴维孙和革末的单晶衍射实验



C. J. Davisson
(1881–1958)



L. H. Germer
(1896–1971)

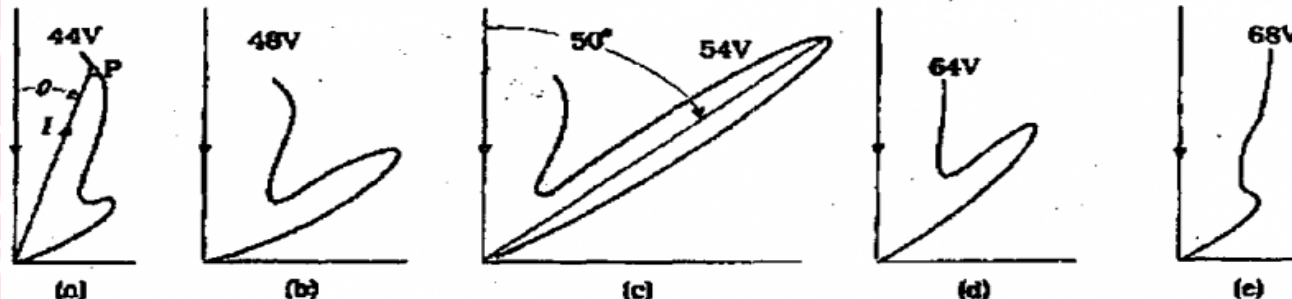


Fig. 12.10

C. Davisson, L.H. Germer "Reflection of electrons by a crystal of nickel". *Nature* 119 (1927). 558–56



1927, G. P. Thomson利用电子束透射金属箔得到衍射照片

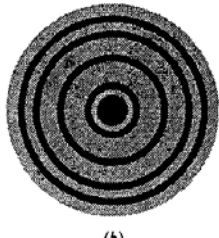
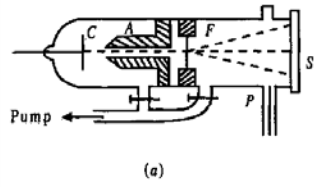
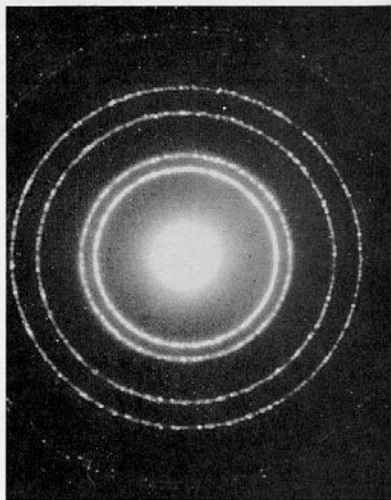
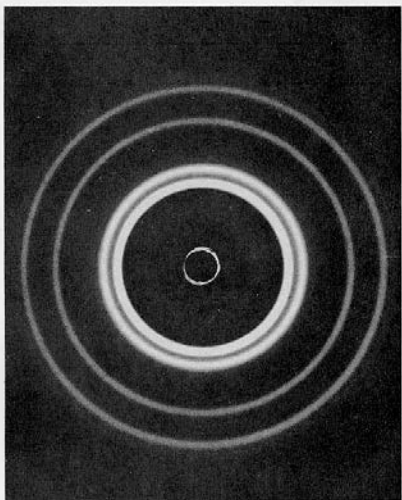
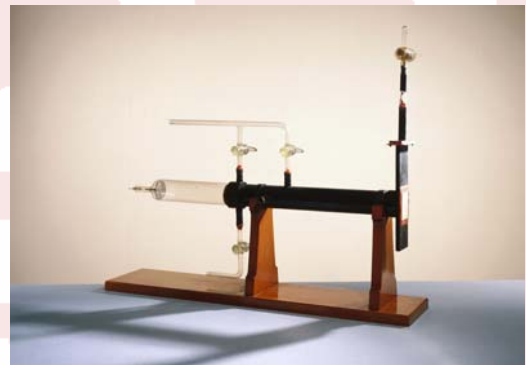


Fig. 29.5

The diffraction pattern on the left was made by a beam of x rays passing through thin aluminum foil. The diffraction pattern on the right was made by a beam of electrons passing through the same foil.

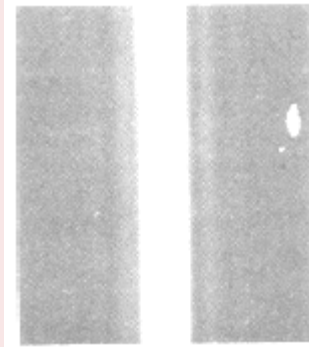
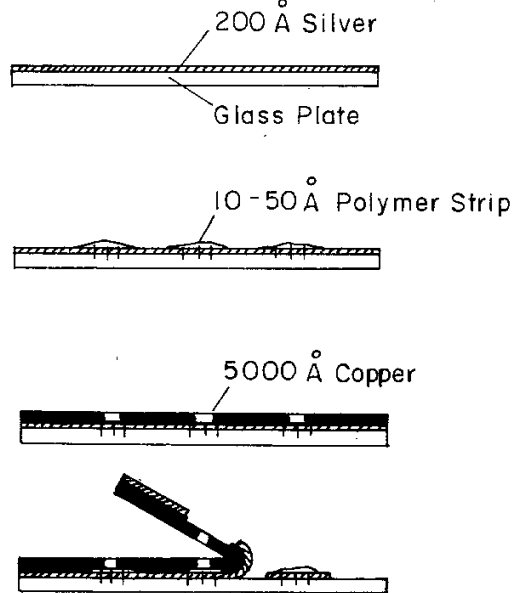


G. P. Thomson
(1892 – 1975)

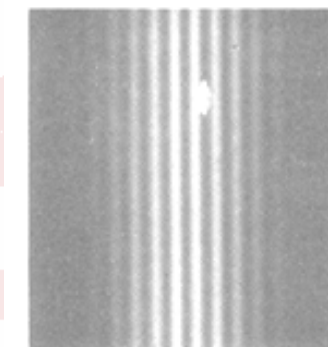




1961, V. C. Jönsson的电子单缝和多缝实验



单缝照片



双缝照片

The most beautiful experiment in physics
Voted by readers of Physics Today in 2002

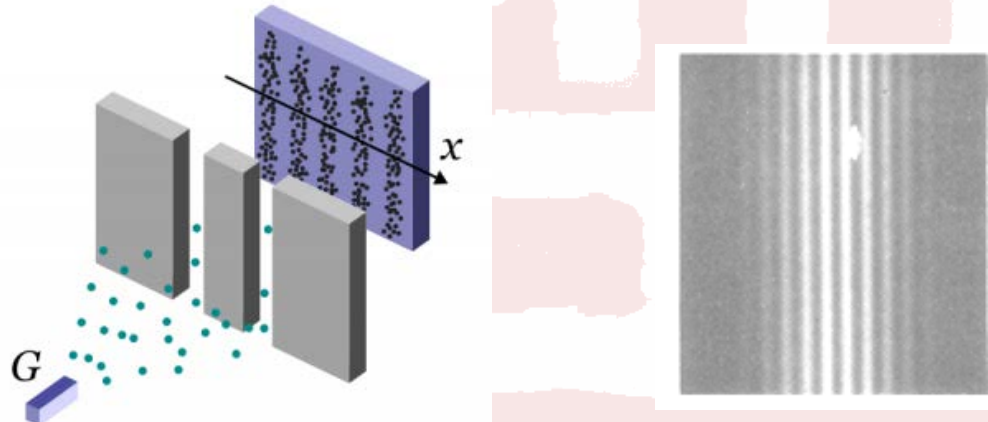
V. C. Jönsson, Z. Phys., 161(1961) 454



Particle - wave duality of matter particles

plays key role in quantum mechanics

electron Young's double-slit experiment



The most beautiful experiment in physics
Voted by readers of Physics World in 2002

C. Jönsson, Z. Phys., 161(1961) 454

原子干涉仪

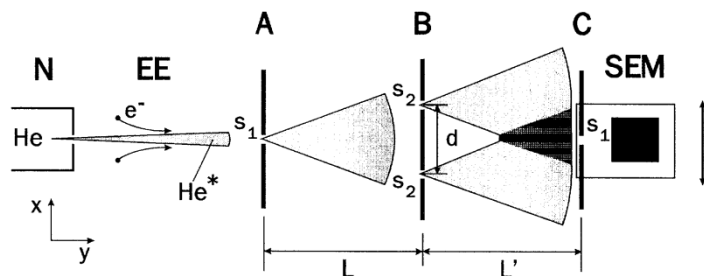


FIG. 2. Schematic representation of the experimental setup: nozzle system and gas reservoir N; electron impact excitation EE; entrance slit A, double slit B, and detector screen C; secondary electron multiplier SEM (mounted together with C on a translation stage). Dimensions: $d = 8 \mu\text{m}$, $L = L' = 64 \text{ cm}$; slit widths: $s_1 = 2 \mu\text{m}$, $s_2 = 1 \mu\text{m}$.

$$T = 295 \text{ K} \quad E_k = \frac{3}{2} k_B T \sim 0.038 \text{ eV}$$

$$\lambda = \frac{hc}{\sqrt{2Mc^2E_k}} \sim 0.073 \text{ nm}$$

$$T = 83 \text{ K} \quad E_k = \frac{3}{2} k_B T \sim 0.011 \text{ eV}$$

$$\lambda = \frac{hc}{\sqrt{2Mc^2E_k}} \sim 0.14 \text{ nm}$$

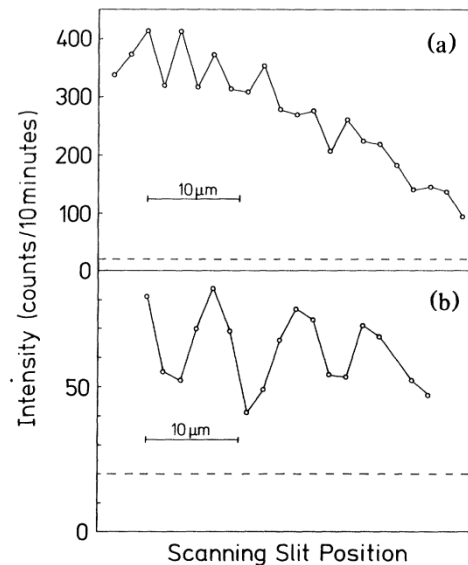
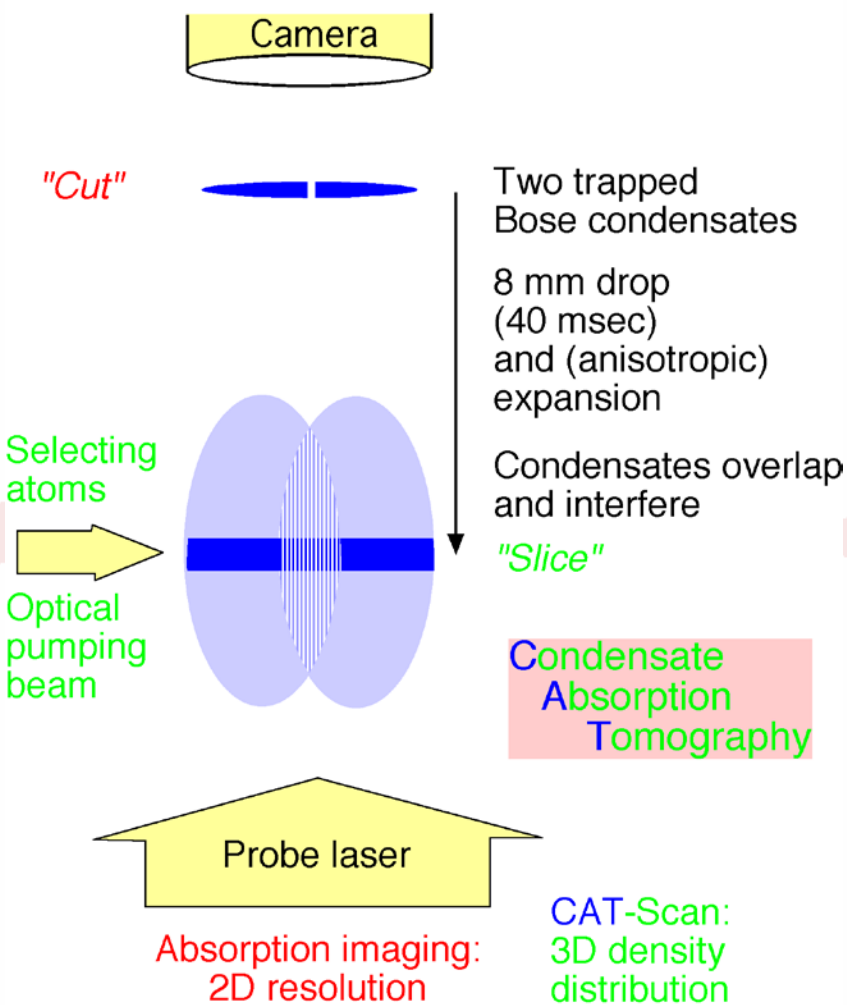


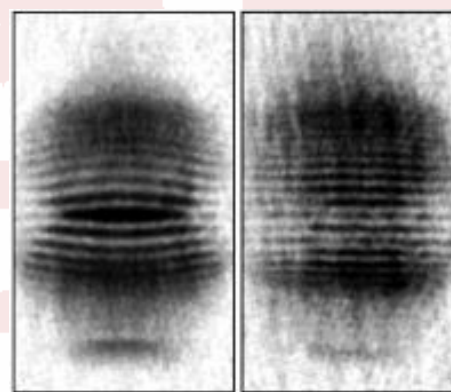
FIG. 4. Measured atomic intensity profiles in the detector plane as a function of the lateral detector position x . The profile is probed with the $2\text{-}\mu\text{m-wide single slit}$. Atomic wavelength (a) $\lambda_{dB} = 0.56 \text{ \AA}$ and (b) $\lambda_{dB} = 1.03 \text{ \AA}$. The number of detected atoms during 10 min is plotted on the vertical axis. The dashed line is the detector background, with the atomic beam blocked in front of the entrance slit. The line connecting the experimental data is a guide to the eye.



Interference of two condensates



Wolfgang Ketterle

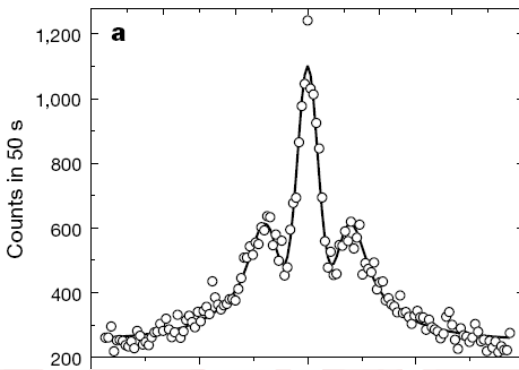
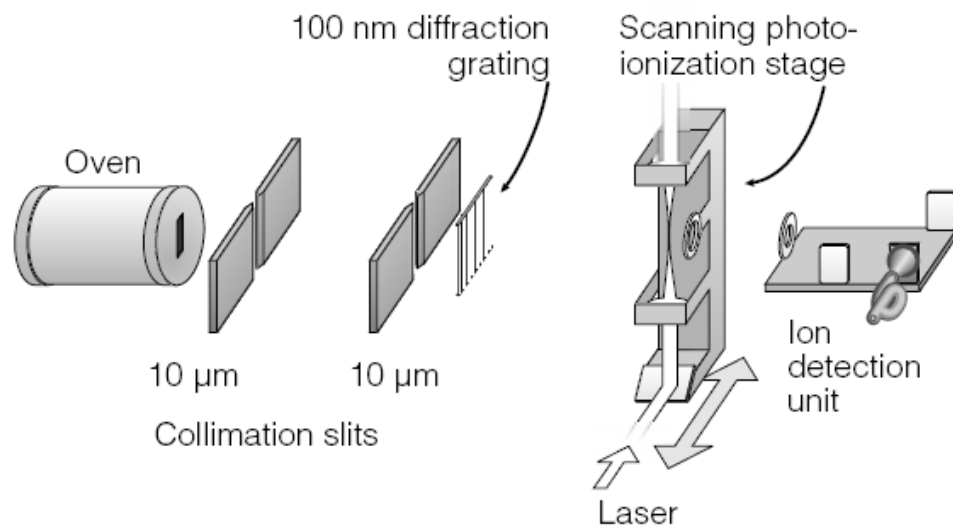




Wave-particle duality of C₆₀ molecules

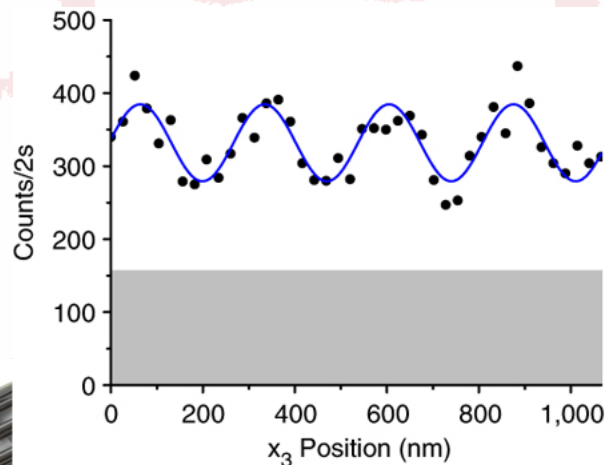
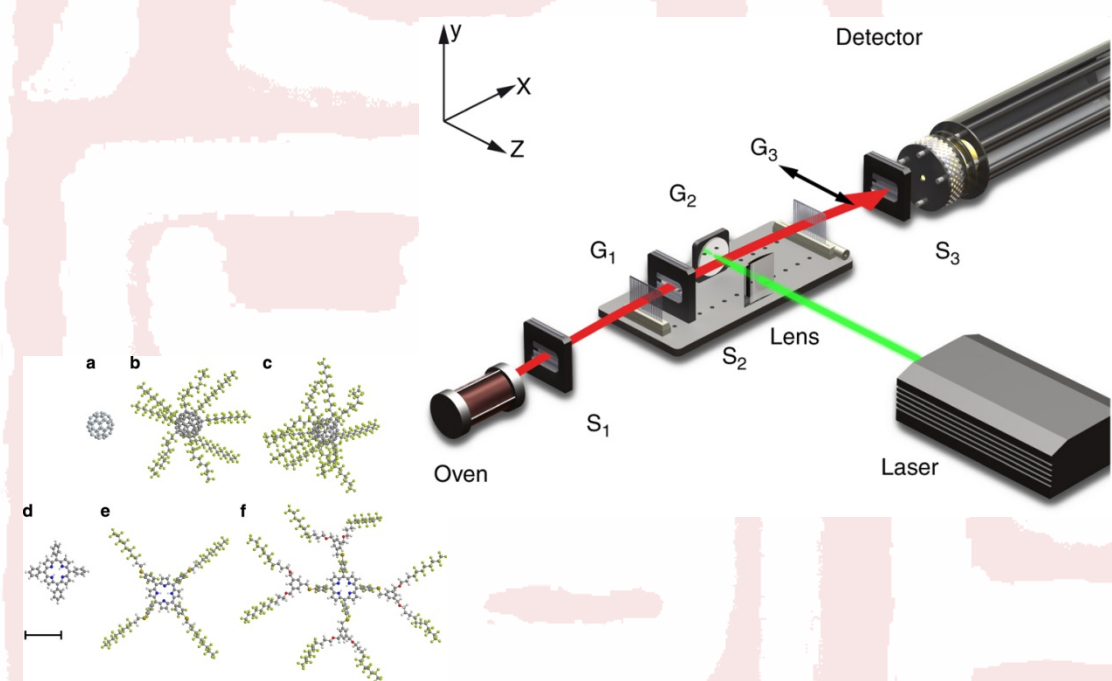
NATURE | VOL 401 | 14 OCTOBER 1999 |

Markus Arndt, Olaf Nairz, Julian Vos-Andreae, Claudia Keller,
Gerbrand van der Zouw & Anton Zeilinger



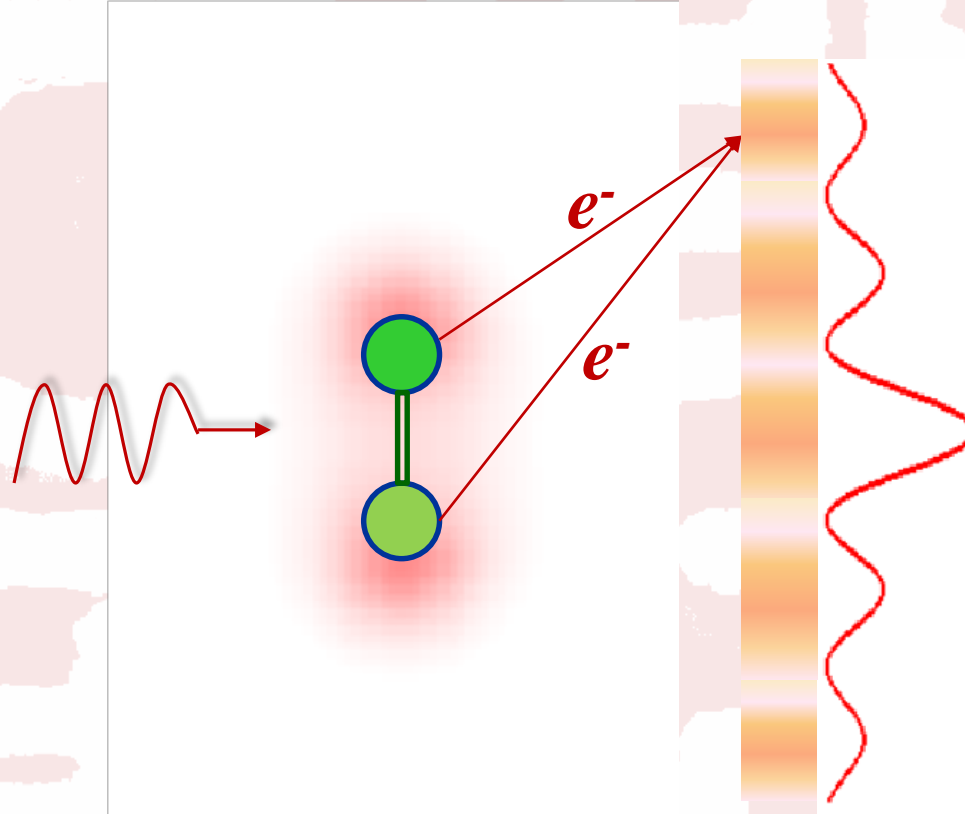
Quantum interference of large organic molecules

Gerlich, S. et al. *Nature Commun.* **2**, 263 (2011).





Molecular double-slit interference



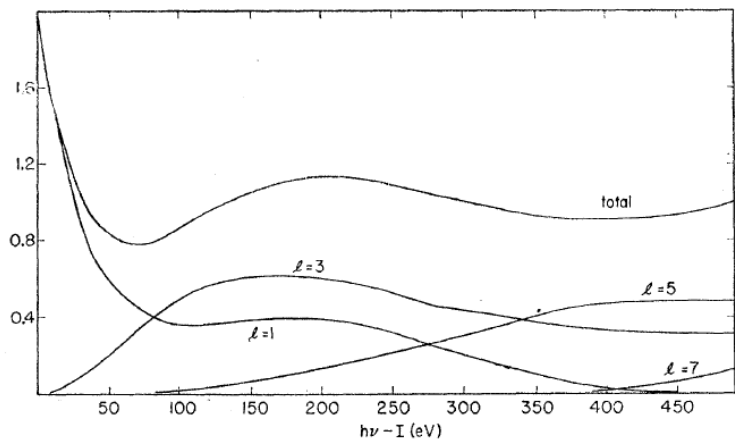
Coherent superposition of electrons emitted from two atoms in diatomic molecules can be regarded as a molecular double-slit



Molecular double-slit interference

Photoionization of N₂ and O₂

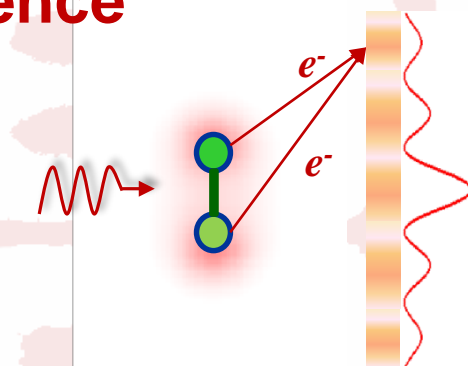
H. D. Cohen and U. Fano *Phys. Rev.* **150** 30 (1966)



$$\sigma = \sigma_0 \left[1 + \frac{\sin(k_e R_e)}{k_e R_e} \right]$$

where σ_0 is an atomic photoionization cross section, k_e is the electron-wave vector and R_e is the internuclear distance at equilibrium.

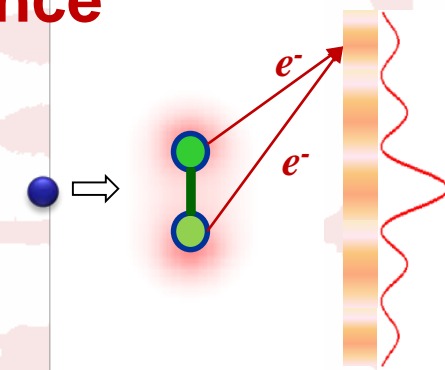
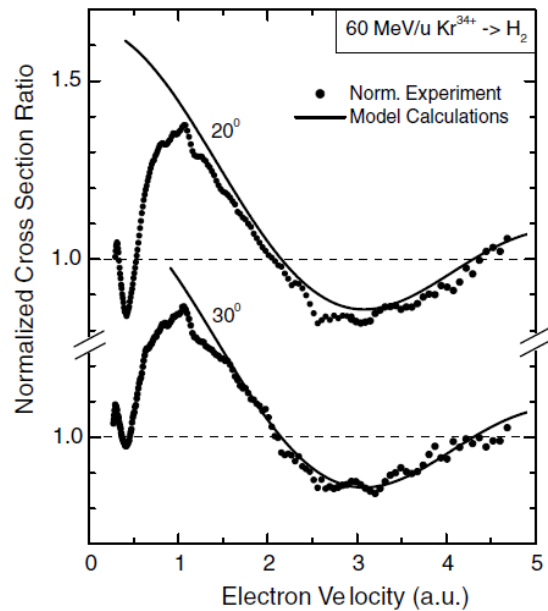
Such interference effects, arising from the coherent emission of electrons from two indistinguishable atoms, lead to the energy- or angle-dependent oscillations in cross sections.





Molecular double-slit interference

Ionizations by heavy ions

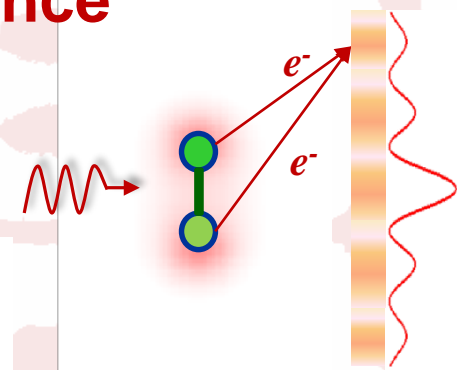
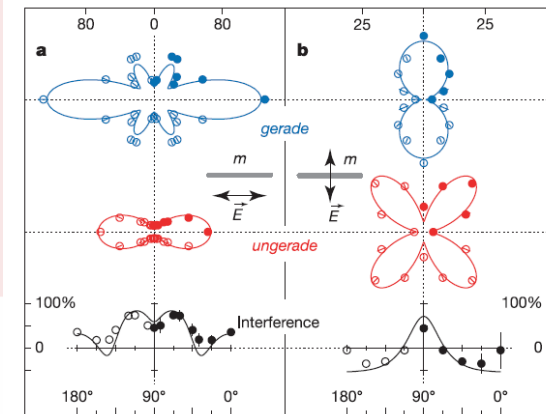
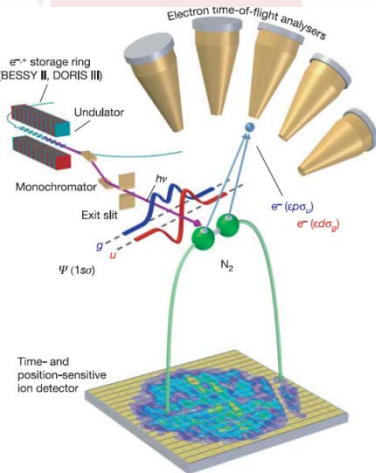


- [1] N. Stolterfoht *et al*, *Phys. Rev. Lett.* **87** 23201 (2001).
- [2] D. Misra, U. Kadhane, Y. P. Singh *et al.*, *Phys. Rev. Lett.* **92**, 153201 (2004).
- [3] H. T. Schmidt, D. Fischer, Z. Berenyi *et al*, *Phys. Rev. Lett.* **101**, 083201 (2008).
- [4] Deepankar Misra, H. T. Schmidt, M. Gudmundsson *et al*, *Phys. Rev. Lett.* **102**, 153201 (2009).
- [5] A. B. Voitkiv, B. Najjari, and D. Fischer, *Phys. Rev. Lett.* **106**, 233202 (2011).



Molecular double-slit interference

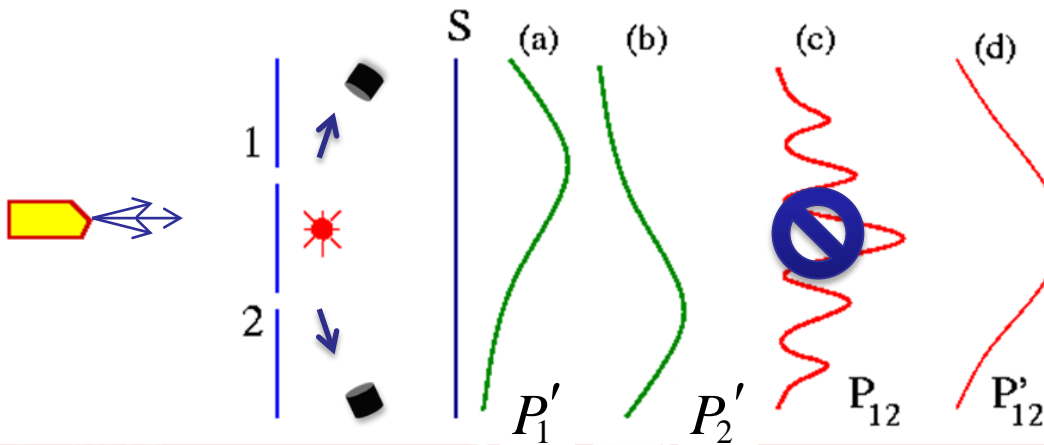
Photoionization of diatomic molecules



- [1] D. Rolles, M. Braune, S. Cvejanović et al., *Nature* **437**, 711 (2005).
- [2] J. Fernández, O. Fojón, A. Palacios, and F. Martín, *Phys. Rev. Lett.* **98**, 043005 (2007).
- [3] D. Akoury, K. Kreidi, T. Jahnke et al., *Science* **318**, 949 (2007).
- [4] K. Kreidi, D. Akoury, T. Jahnke et al., *Phys. Rev. Lett.* **100**, 133005 (2008).
- [5] B. Zimmermann, D. Rolles, B. Langer et al., *Nature Physics* **4**, 649 (2008).
- [6] S. E. Canton, E. Plésiat, J. D. Bozek et al., *PNAS* **108**, 7302 (2011).
- [7] R. K. Kushawaha, M. Patanen, R. Guillemin et al., *PNAS* **110**, 15201 (2013).



Knowing which way



Richard Feynman
(1918-1988)

电子散射一个光子：实验上可以确定电子穿过1还是穿越2 (“thought experiment”)

跟踪电子

电子穿过1，记录到 P'_1 \rightarrow 类似于遮上缝2的分布 P_1

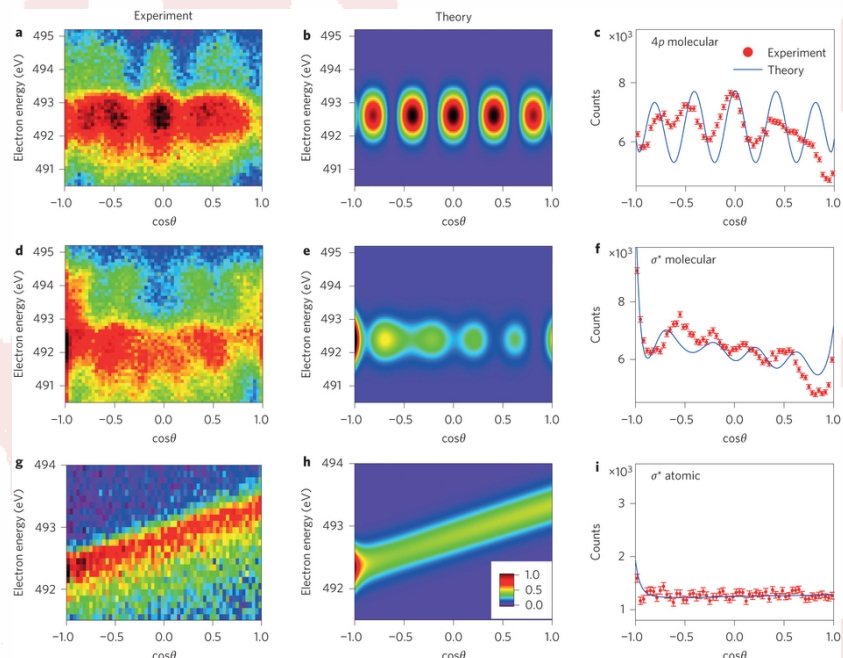
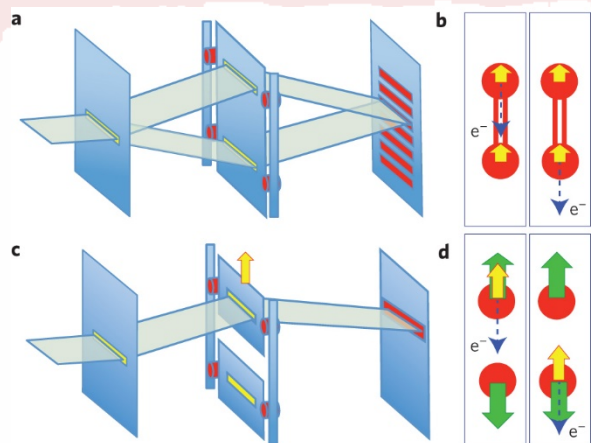
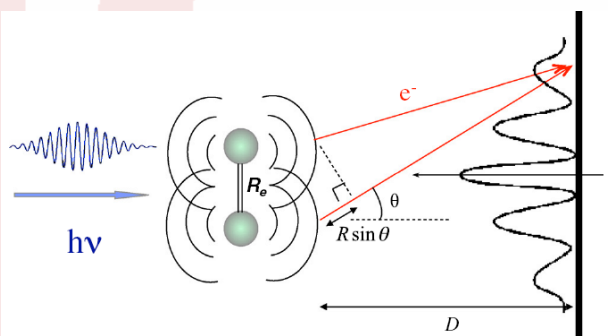
电子穿过2，记录到 P'_2 \rightarrow 类似于遮上缝1的分布 P_2

“看”到的穿过1的电子的分布应该与关不关闭缝2无关。

我们看到的总概率分布 $P'_{12} = P'_1 + P'_2$

我们看到了电子穿过哪个狭缝，但我们却丢失了干涉图像。

Knowing which way



Einstein–Bohr recoiling double-slit gedanken experiment performed at the molecular level

Nature Photonics 9, 120 (2015)



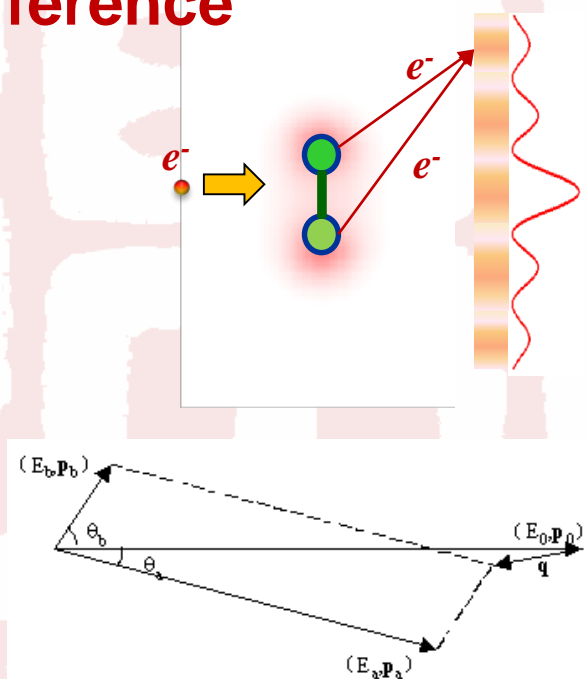
Molecular double-slit interference

Electron impact ionization of H₂

Two Effective Center (TEC) approximation
Or
Plane Wave approximation

$$\psi = \frac{1}{\sqrt{2}} (1s_A + 1s_B)$$

$$\sigma^{(3)} = \frac{d^3\sigma}{d\Omega_e d\Omega_s dE_e} \cong 2[1 + \sin(\chi R_e) / (\chi R_e)] \sigma_A^{(3)}$$

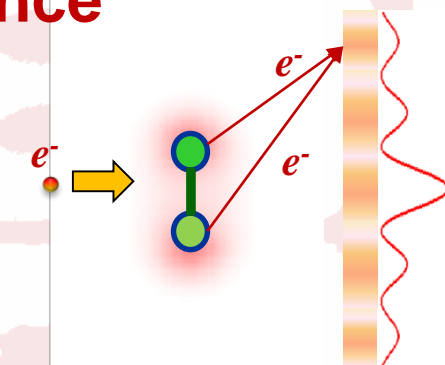
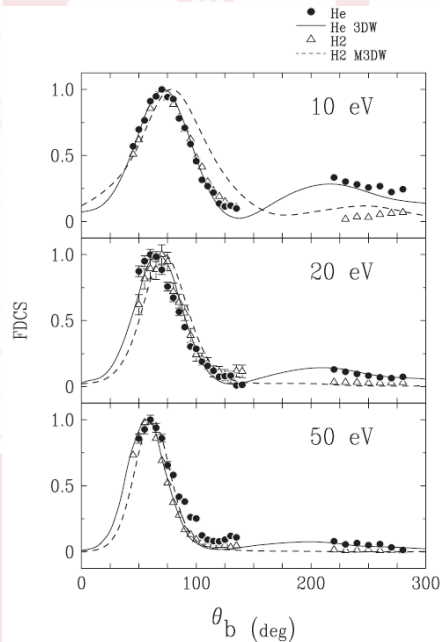
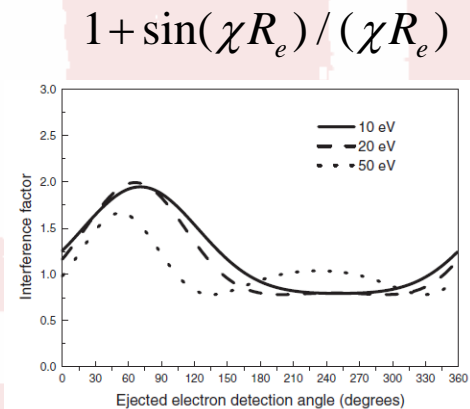


- [1] C. R. Stia, O. A. Fojn, P. F. Weck et al., Phys. Rev. A 66, 052709 (2002).
- [2] D. S. Milne-Brownlie, M. Foster, J. Gao et al., Phys. Rev. Lett. 96, 233201 (2006).
- [3] O. Kamalou, J.Y. Chesnel, D. Martina et al., Phys. Rev. A 71, 010702(R) (2005).
- [4] E. M. Staicu-Casagrande et al., J. Phys. B 41, 025204 (2008).
- [5] Z. N. Ozer, H. Chaluvadi, M. Ulu et al., Phys. Rev. A 87, 042704 (2013).



Molecular double-slit interference

Electron impact ionization of H₂



The interference effect was revealed from the suppression or enhancement of the forward (binary) or backward (recoil) scattering peaks as compared to helium at same kinematics.

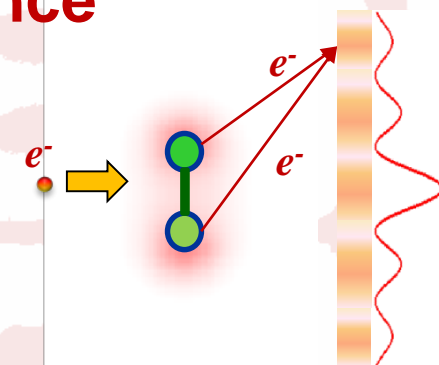
- [1] C. R. Stia, O. A. Fojn, P. F. Weck et al., J. Phys. B 36, L257 (2003).
- [2] D. S. Milne-Brownlie, M. Foster, J. Gao et al., Phys. Rev. Lett. 96, 233201 (2006).
- [3] O. Kamalou, J.Y. Chesnel, D. Martina et al., Phys. Rev. A 71, 010702(R) (2005).
- [4] E. M. Staicu-Casagrande et al., J. Phys. B 41, 025204 (2008).
- [5] Z. N. Ozer, H. Chaluvadi, M. Ulu et al., Phys. Rev. A 87, 042704 (2013).



Molecular double-slit interference

Electron impact ionization of H₂

Can we observe Young-type interference
in binary (e,2e)?



Binary (e, 2e) process



$$\frac{d^3\sigma}{dE_a d\Omega_a d\Omega_b} \propto \int d\Omega_p \left| \psi_j(p) \right|^2$$

coincidence

取向平均



For ground state of H₂ molecule

$$\psi = \frac{1}{\sqrt{2}}(1s_A + 1s_B)$$

$$\rightarrow \sigma^{(3)} \cong 2[1 + \sin(\chi R_e) / (\chi R_e)]\sigma_H^{(3)}$$

@ EMS: $\chi = p_0 - K = -q = p$

$$\rightarrow \sigma_{EMS}^{(3)} \cong 2[1 + \sin(pR_e) / (pR_e)]\sigma_H^{(3)}$$

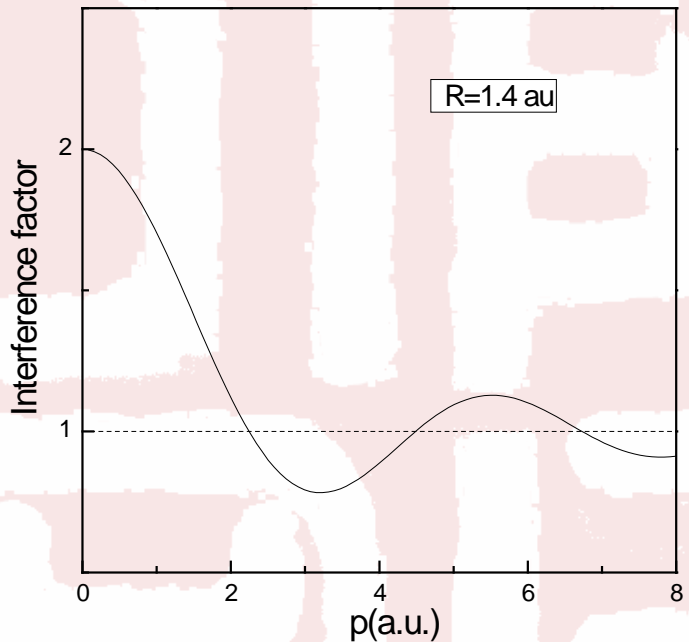
→ Interference factor

$$\frac{\sigma_{EMS}^{(3)}}{2\sigma_H^{(3)}} \cong 1 + \sin(pR_e) / (pR_e)$$



For ground state of H_2 molecule

$$R_e = R_{HH} = 1.4 \text{ a.u.}$$

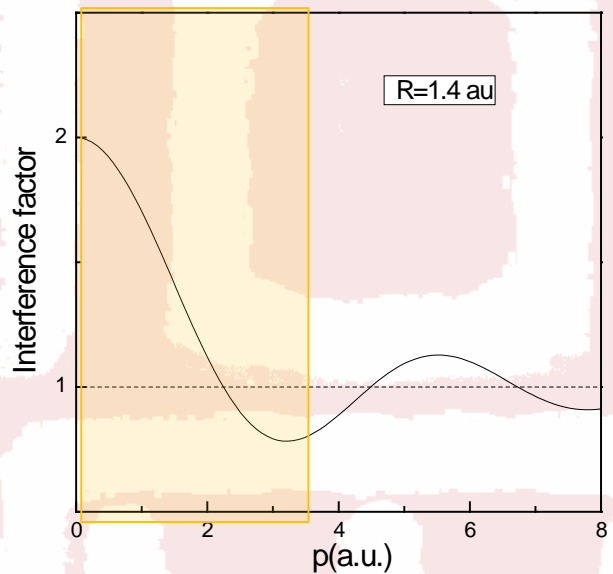


$$\frac{\sigma_{EMS}^{(3)}}{2\sigma_H^{(3)}} \simeq 1 + \sin(pR_e) / (pR_e)$$

We can directly observe the interference factor

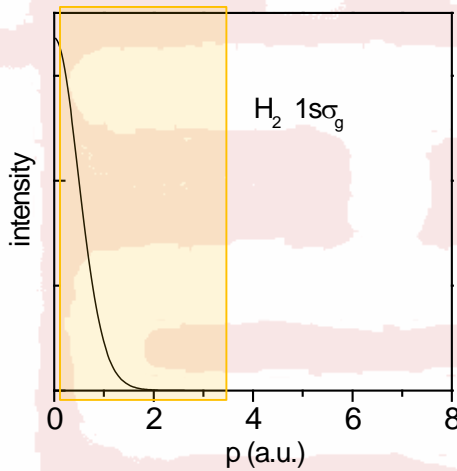


However, for H_2 , it is difficult.



- (1) momentum range $0 \sim 3.5$ a.u.
- (2) intensity of EMS cross section decreases very rapidly.

$$\frac{\sigma_{EMS}^{(3)}}{2\sigma_H^{(3)}} \cong 1 + \sin(pR_e)/(pR_e)$$





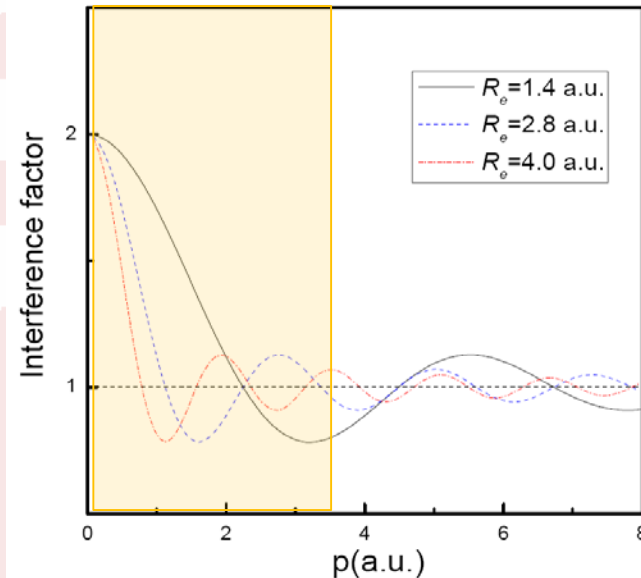
➤ larger internuclear distance

$$\frac{\sigma_{EMS}^{(3)}}{2\sigma_H^{(3)}} \approx 1 + \sin(pR_e)/(pR_e)$$

The oscillation period $\sim 2\pi/R_e$

$R_e = 4.0$ a.u., the period ~ 1.6 a.u.

$R_e = 1.4$ a.u., the period ~ 4.5 a.u.



(e, 2e) of CF_4

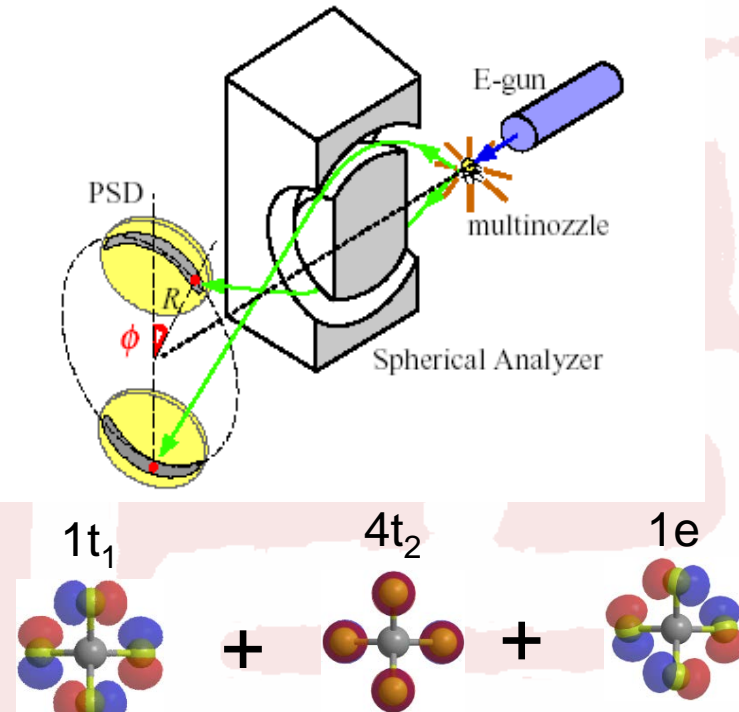
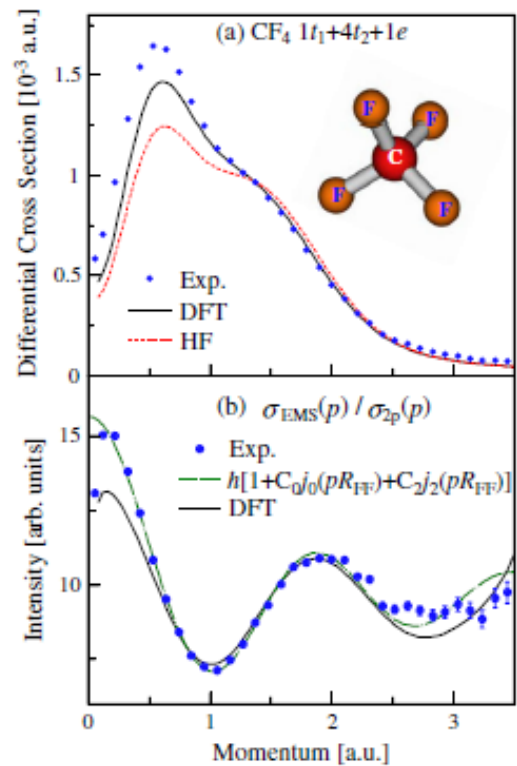


中国科学技术大学

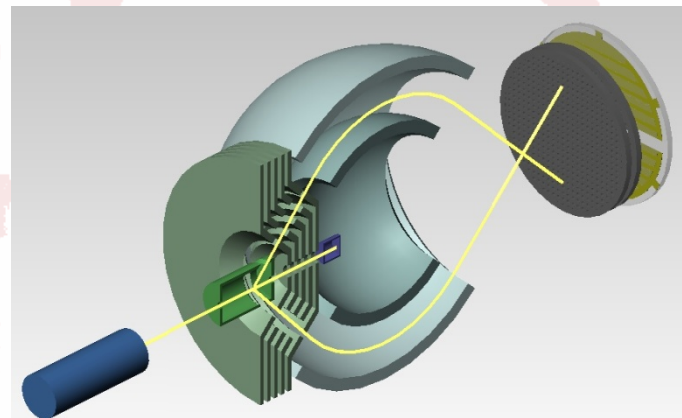
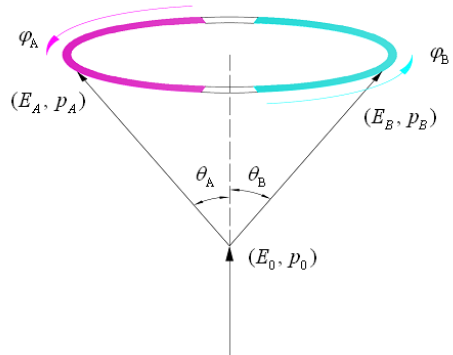
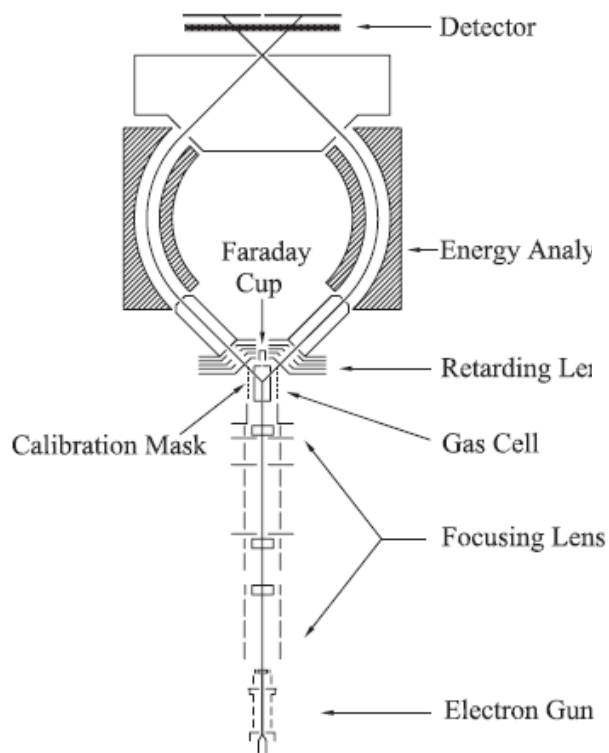


For CF_4 , $R_e = 4.02 \text{ a.u.}$

$$\sigma_{\psi_i(p)} / \sigma_{F_2 p(p)} = \text{const} \times [1 + a_0 j_0(pR_{F-F}) + a_2 j_2(pR_{F-F})]$$



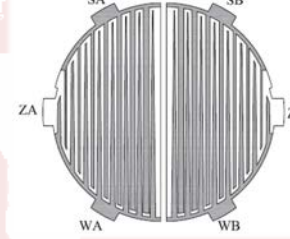
N. Watanabe *et al*, Phys. Rev. Lett. 108, 173201 (2012)



**Non-coplanar
symmetric geometry**

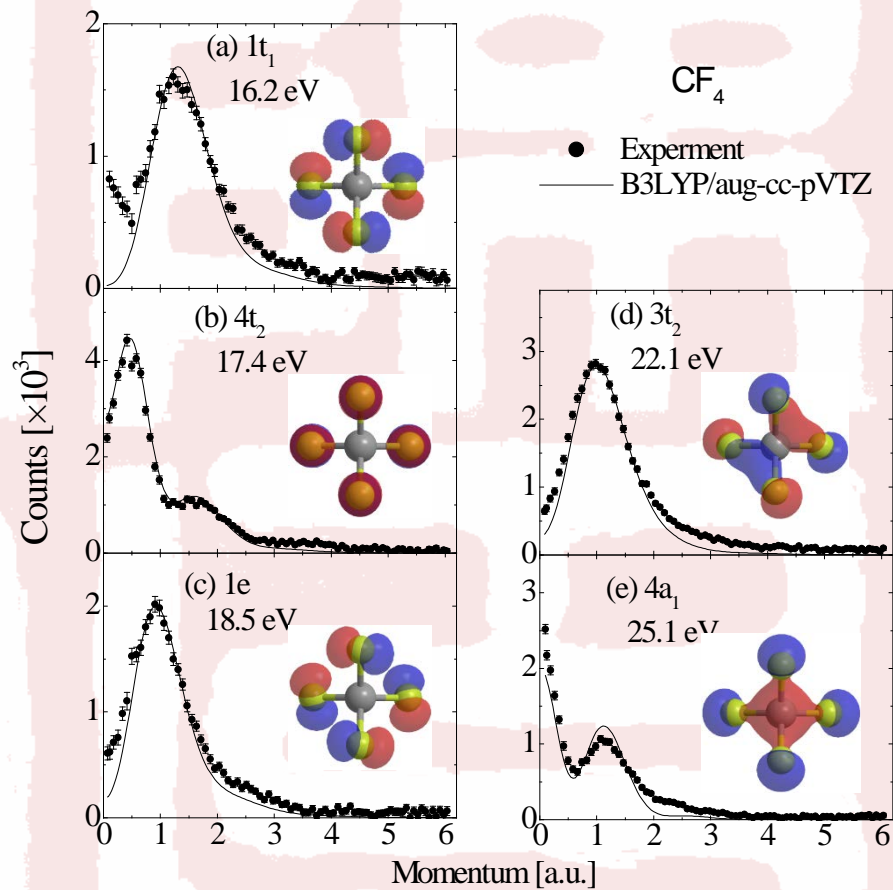
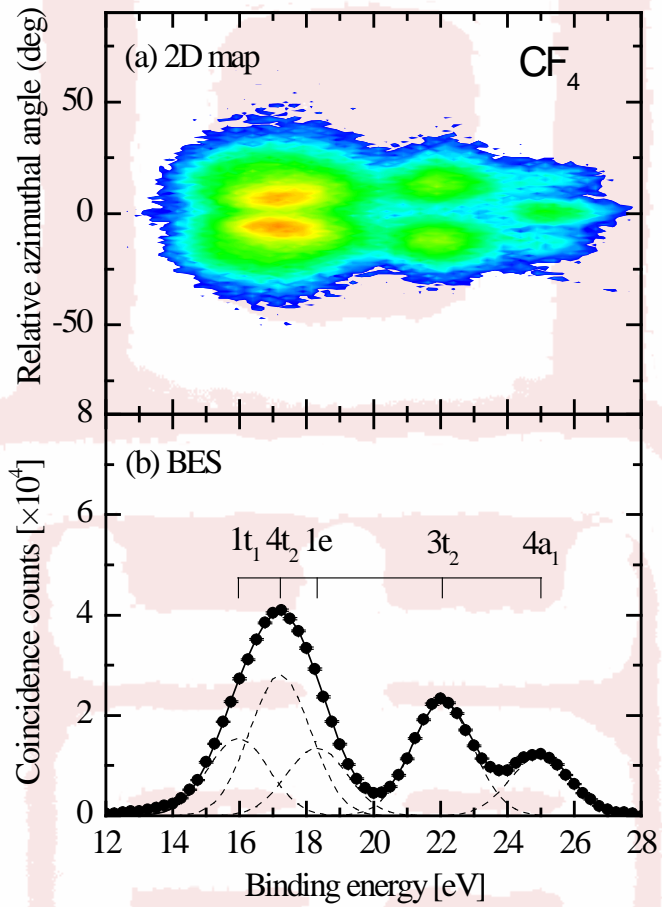
$$E_a = E_b$$

$$\theta_a = \theta_b = 45^\circ$$



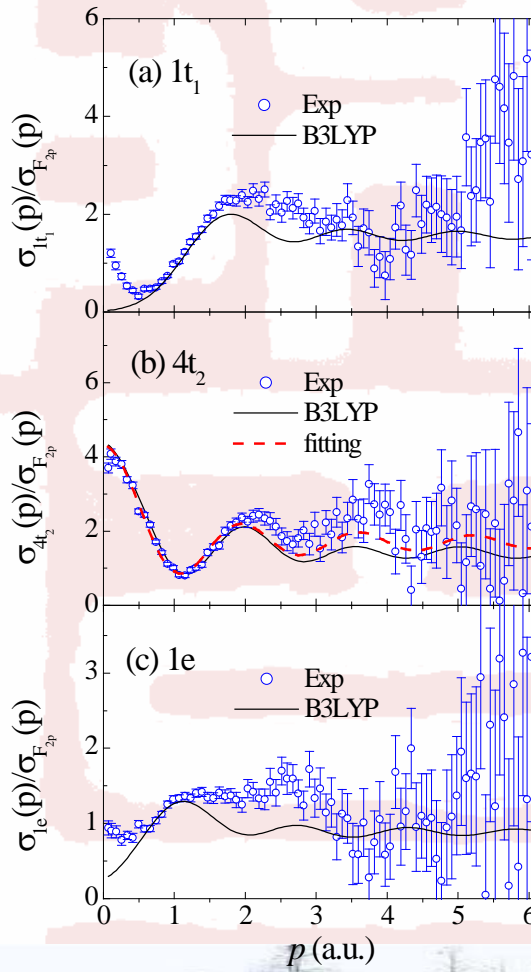
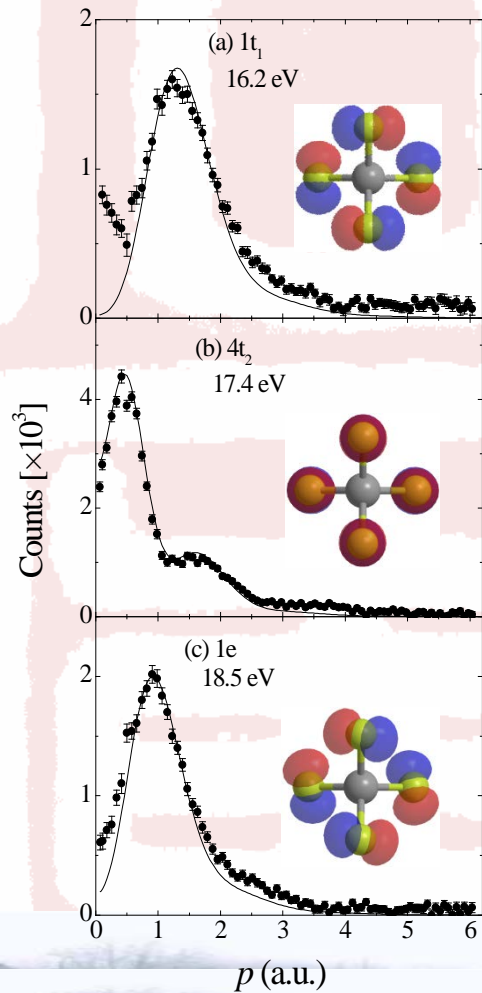
A high-sensitivity angle and energy dispersive multichannel electron momentum spectrometer with 2π angle range

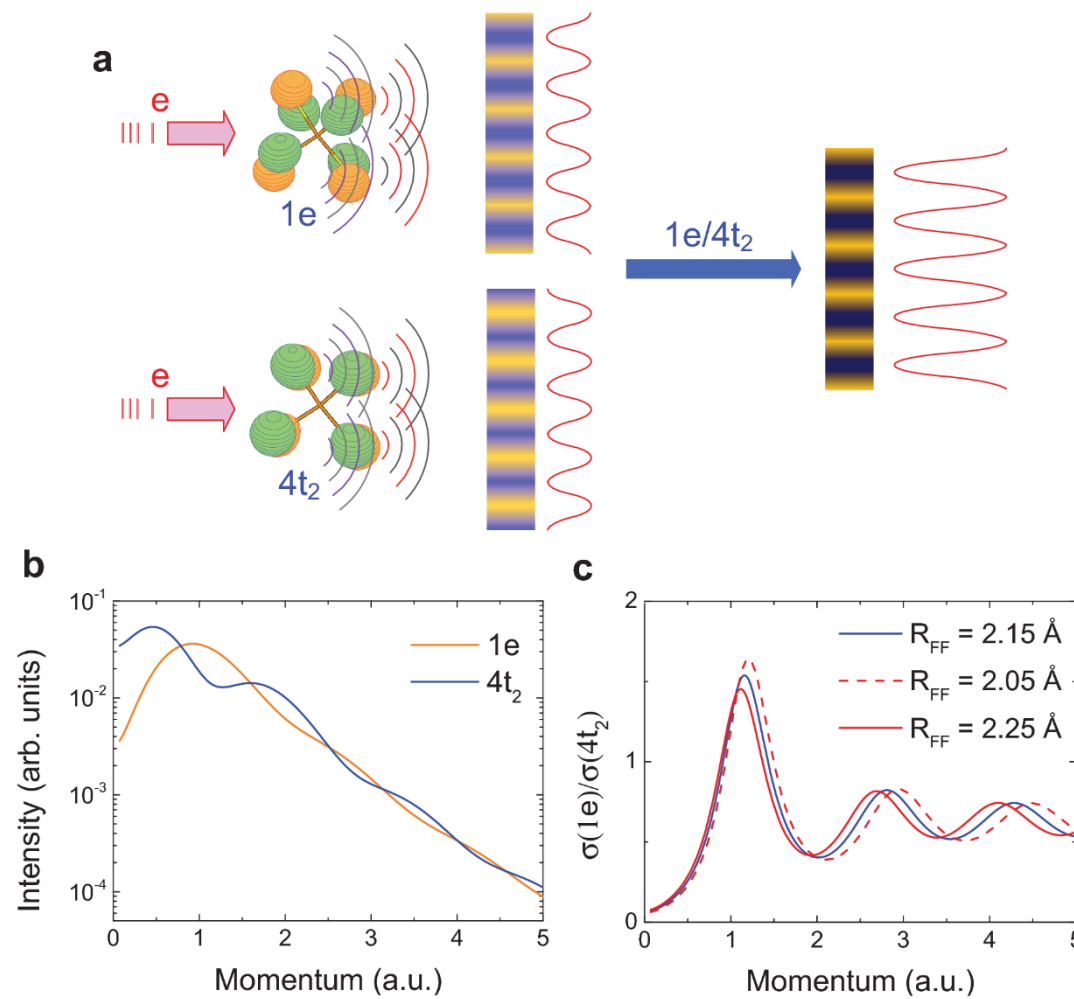
Electron Momentum Spectroscopy of CF_4



Observing the multicenter interference patterns with more periods at extended momentum range

$$\sigma_{\psi_i(p)} / \sigma_{F_{2p}(p)} = \text{const} \times [1 + a_0 j_0(pR_{F-F}) + a_2 j_2(pR_{F-F})]$$

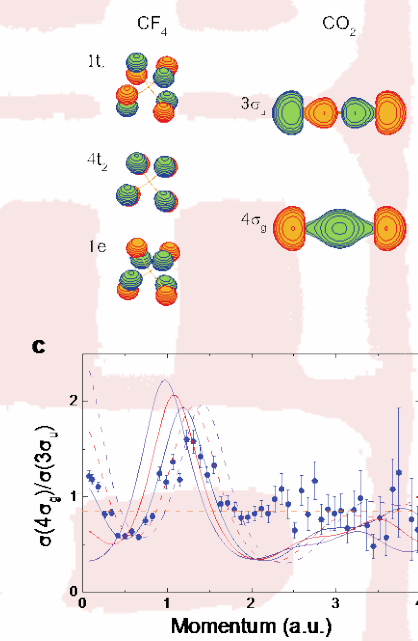
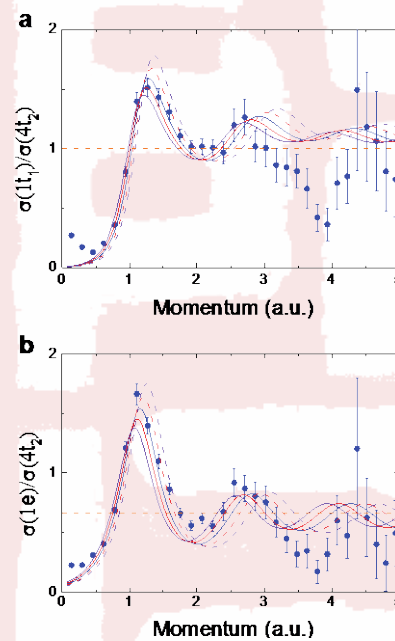
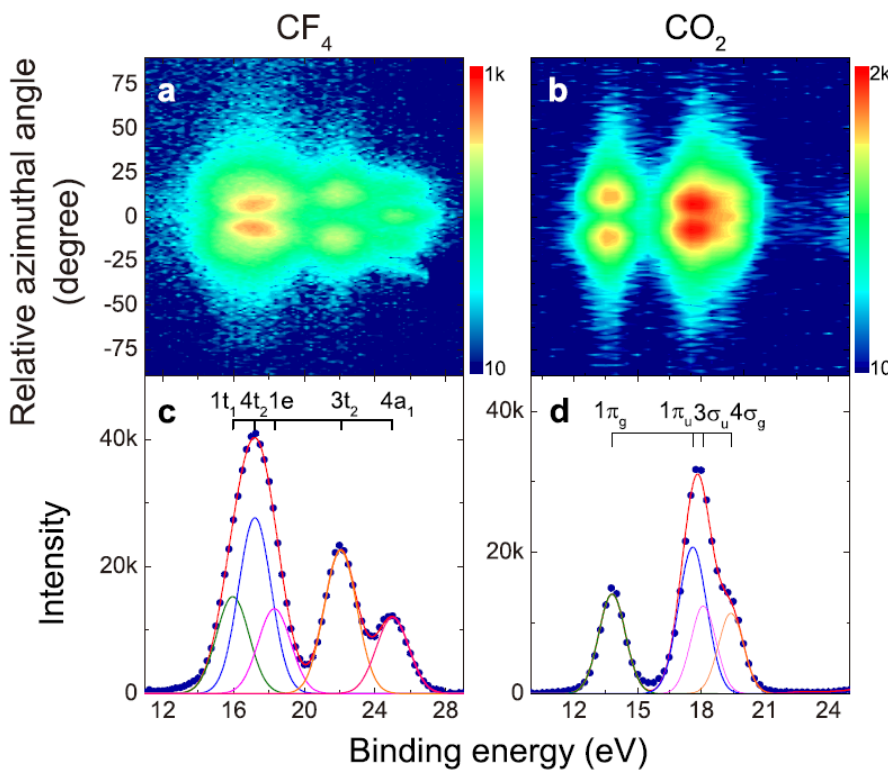


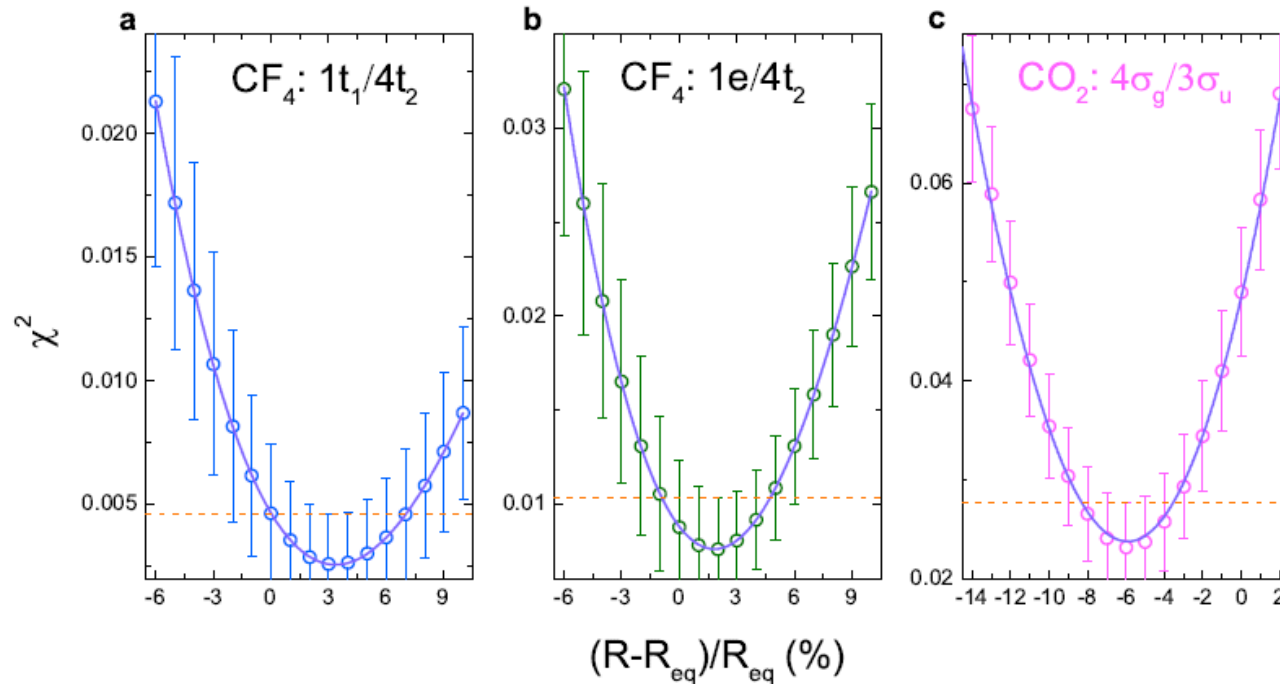


(e, 2e) of CF_4



中国科学技术大学



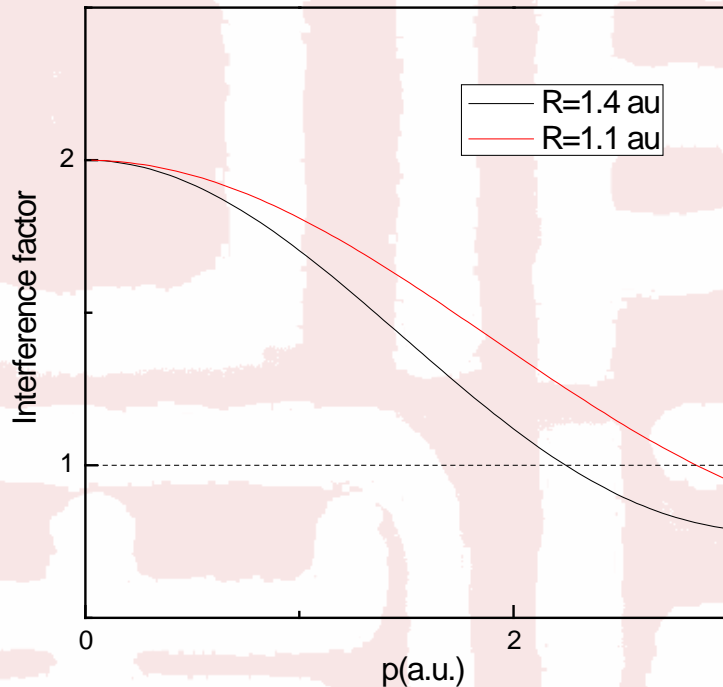


$$R_{\text{FF}} = 2.21 \text{ \AA} \pm 0.07 \text{ \AA}$$

$$R_{\text{OO}} = 2.19 \text{ \AA} \pm 0.07 \text{ \AA}$$



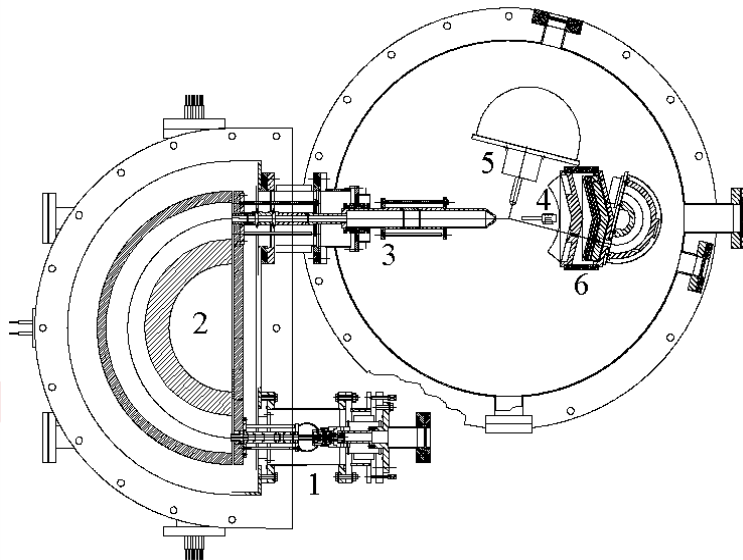
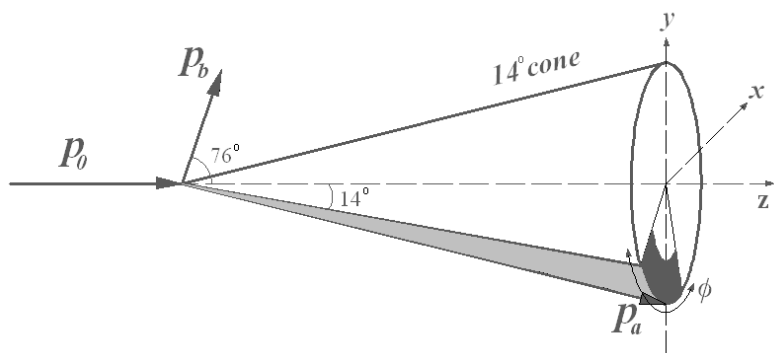
- compare interference factor at different internuclear distance



To observe the movement of the interference fringe



Angular and energy dispersive multi-channel electron momentum spectrometer



Non-coplanar non-symmetric geometry: larger cross section

$$E_0 = 2500 \text{ eV} + \varepsilon_f, E_a \approx 2354 \text{ eV}, E_b \approx 146 \text{ eV}$$

J.Chem.Phys. 125 (2006) 154307

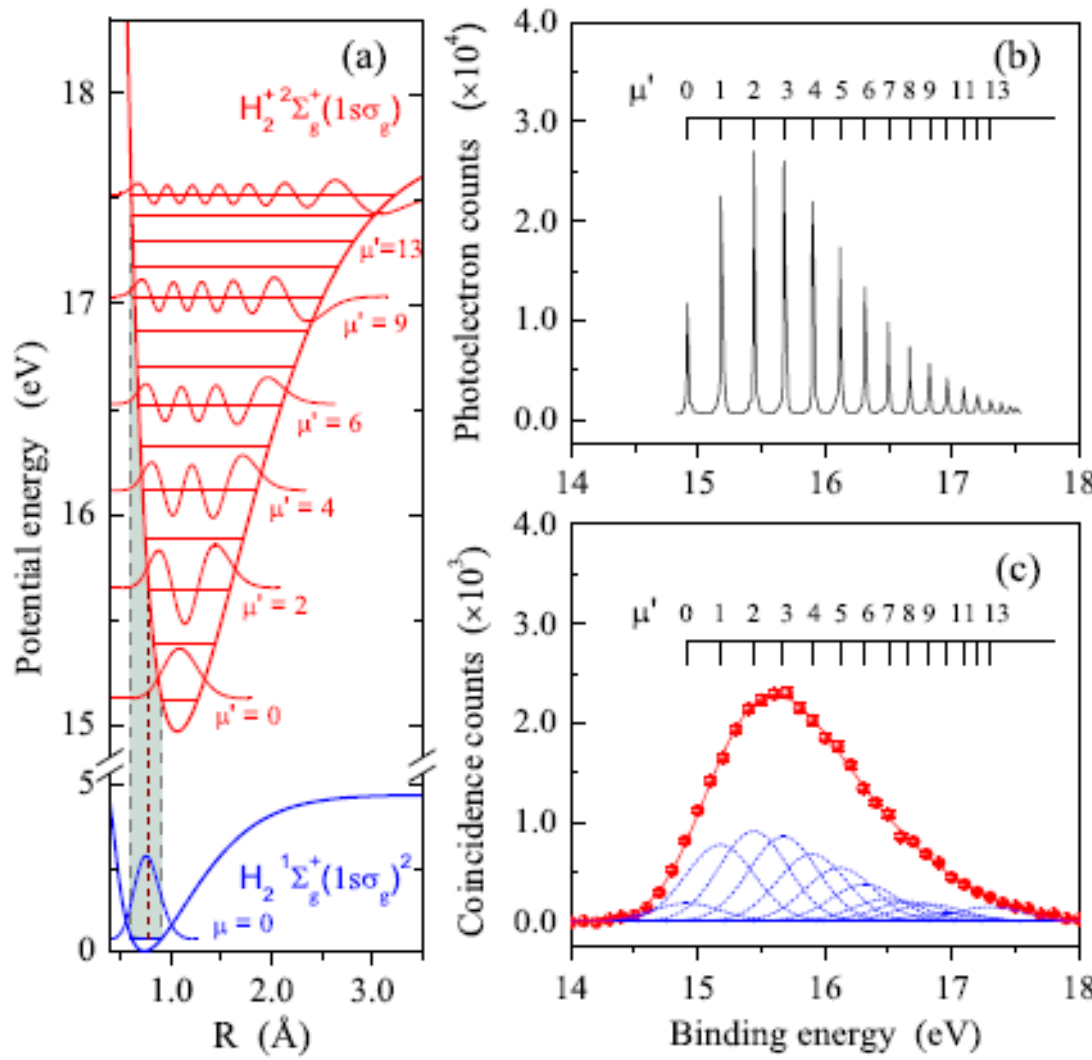
能量分辨: $\Delta E \sim 0.60 \text{ eV}$

动量分辨: $\Delta p \sim 0.10 \text{ a.u.}$

Vibrationally resolved (e , $2e$) of H_2



中国科学技术大学



Zhe Zhang *et al.* Phys. Rev. Lett. 112, 023204 (2014)

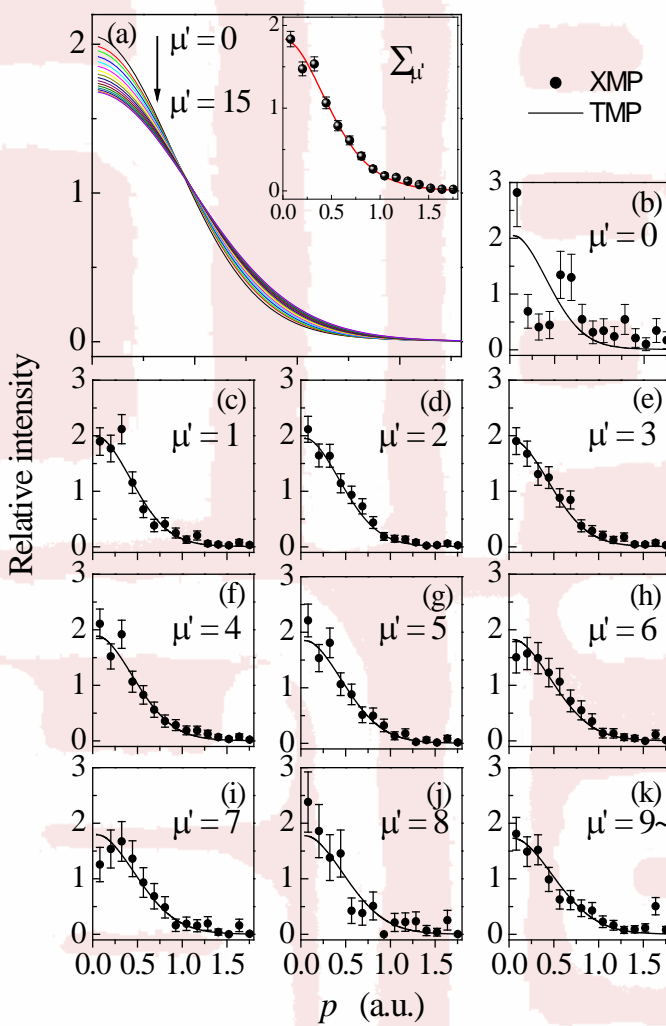
Vibrationally resolved (e , $2e$) of H_2



中国科学技术大学



Experimental momentum profiles for different vibrational states.



Zhe Zhang *et al.* Phys. Rev. Lett. 112, 023204 (2014)

Vibrationally resolved (e , $2e$) of H_2



中国科学技术大学



To highlight the differences, vibrational ratios of EMS cross sections are plotted.

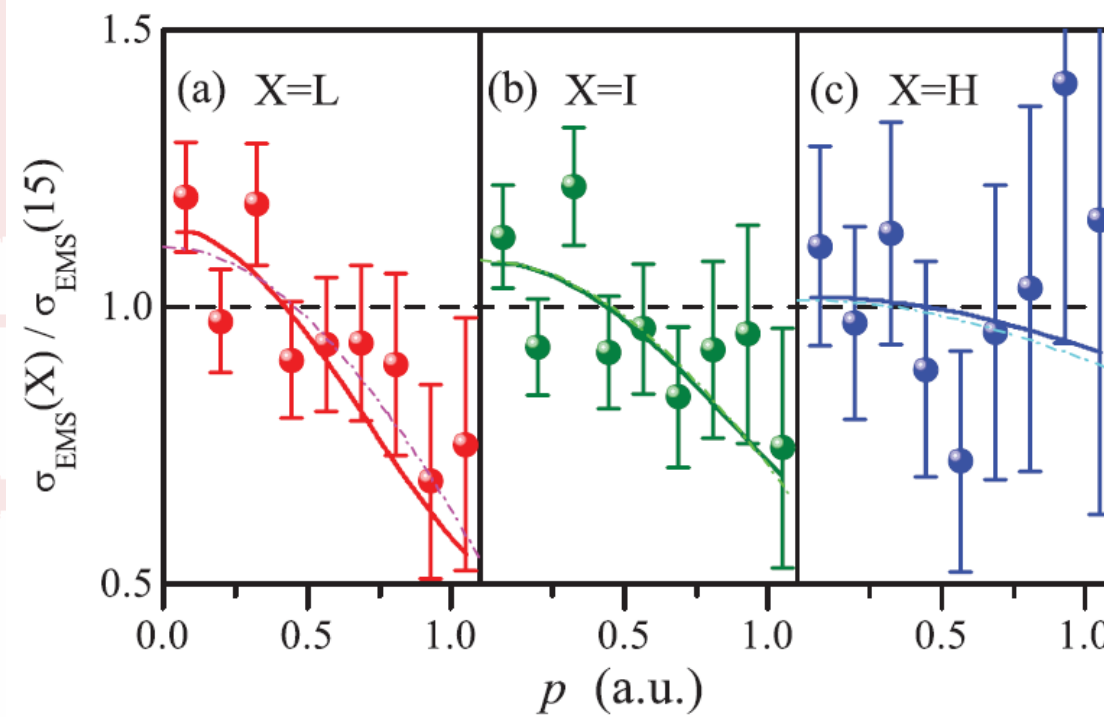
$$\frac{\sigma_{EMS}^{Exp}(X)}{\sigma_{EMS}^{Theo}(\mu' = 15)}$$

$$\frac{\sigma_{EMS}^{Theo}(X)}{\sigma_{EMS}^{Theo}(\mu' = 15)}$$

$$X = H: \mu' > 8$$

$$X = I: \mu' = 4, 5, 6$$

$$X = L: \mu' = 0, 1, 2$$



Zhe Zhang *et al.* Phys. Rev. Lett. 112, 023204 (2014)



$$\langle \mathbf{p} V'_{\mu'} i | 0V_0 \rangle = \int dR X_{\mu'}^*(R) X_0(R) S^{(i)}(R) \varphi(\mathbf{p}, R)$$

$S^{(i)}(R)\varphi(\mathbf{p}, R)$ varies slowly in the range of nuclei coordinate R

V. G. Levin *et al.*, J. Chem. Phys. **63**, 1541 (1975).

$$S^{(i)}(R)\varphi(\mathbf{p}, R) \approx S^{(i)}(R_0)\varphi(\mathbf{p}, R_0)$$

R_0 is the equilibrium internuclear distance

$$\langle \mathbf{p} V'_{\mu'} i | 0V_0 \rangle = (g_0^{\mu'})^{1/2} S^{(i)}(R_0) \varphi(\mathbf{p}, R_0)$$

This implies Franck-Condon principal.

$g_0^{\mu'} = \left| \int dR X_{\mu'}^*(R) X_0(R) \right|^2$ is the Franck-Condon factor.

Zhe Zhang *et al.* Phys. Rev. Lett. **112**, 023204 (2014)

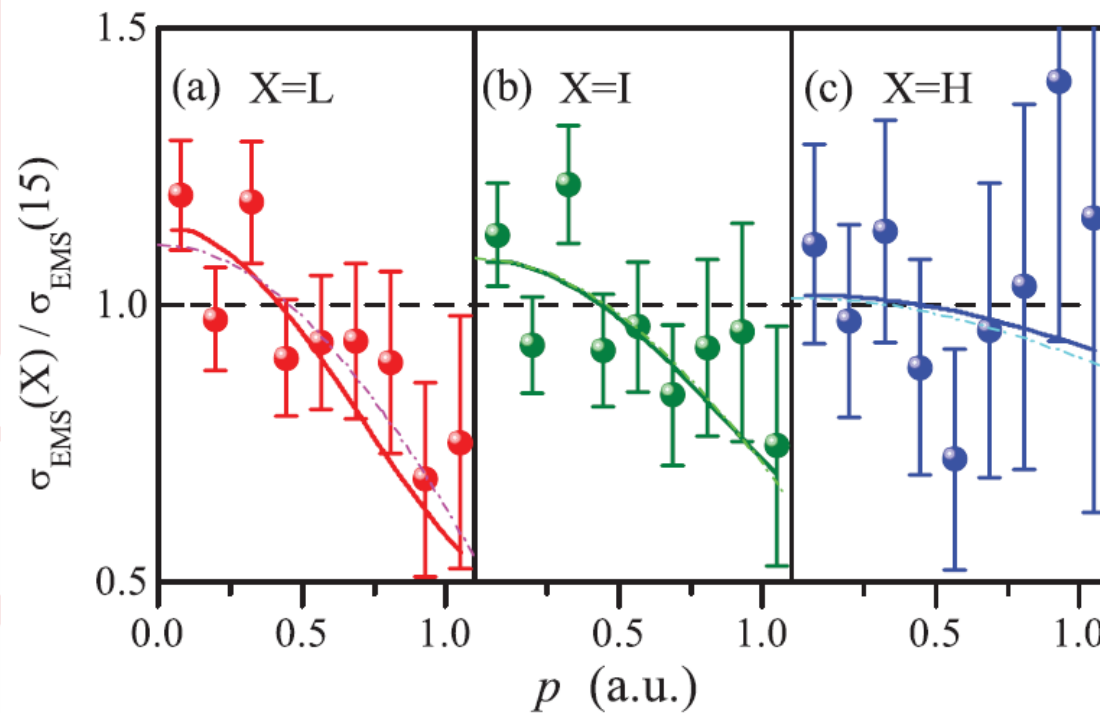
Vibrationally resolved (e , $2e$) of H_2



中国科学技术大学



$$\frac{\sigma_{EMS}(\mu'_1)}{\sigma_{EMS}(\mu'_2)} = \frac{g_0^{\mu'_1}}{g_0^{\mu'_2}} = \text{constant}$$



A: deviations from Franck-Condon approximation.

Zhe Zhang *et al.* Phys. Rev. Lett. 112, 023204 (2014)



The vibrationally resolved cross section can be approximated by

$$\sigma_{EMS}(\mu') = \sigma_0 \left| \int_0^\infty X_{\mu'}(R) \left[1 + \frac{\sin(pR)}{pR} \right]^{1/2} X_0(R) dR \right|^2$$

The vibrational ratio of cross sections can be approximated by

$$\frac{\sigma_{EMS}(\mu_1')}{\sigma_{EMS}(\mu_2')} = \frac{g_0^{\mu_1'}}{g_0^{\mu_2'}} \left[1 + \frac{\delta R_{\mu_1'}}{R_{\mu_2'}} \cos(pR_{\mu_2'}) \right]$$

This formula clearly predicts that the ratio of vibrationally resolved cross sections should oscillate around the quotient of Frank-Condon factors.

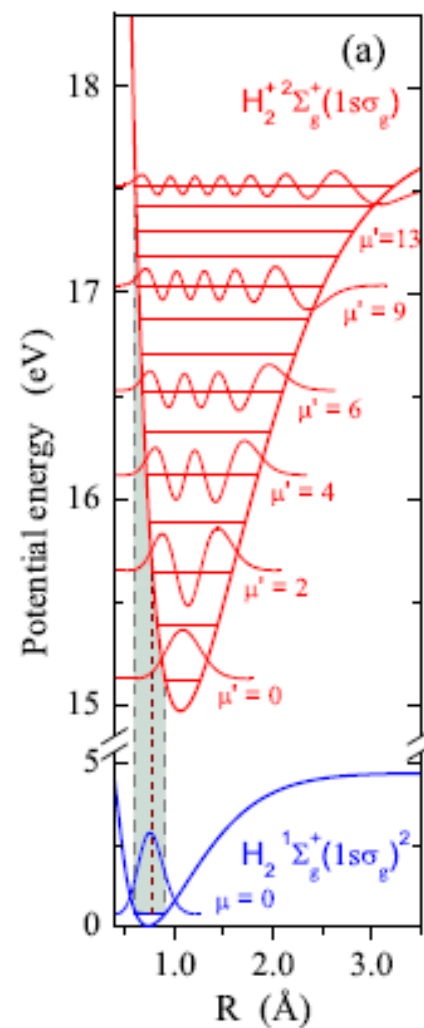
Vibrationally resolved (e , $2e$) of H_2



中国科学技术大学



The turning points are adopted as the characteristic value $R_{\mu'}$

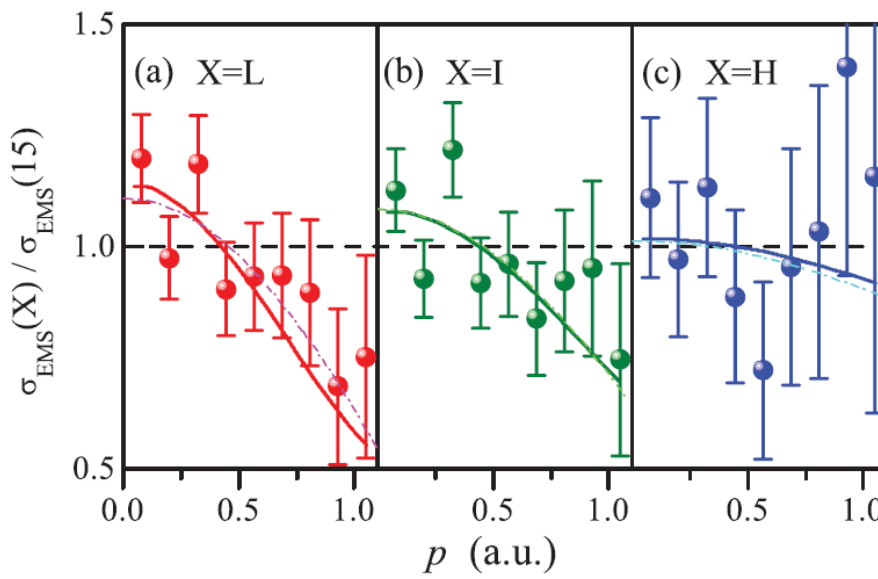


$$\mu' = 15 \quad R_{\mu'} = 1.12 \text{ a.u.}$$

$$X = L, I, H \quad \bar{R}_{\mu'} = 1.6 \text{ a.u.}, \quad 1.35 \text{ a.u.}, \quad 1.15 \text{ a.u.}$$

Fitting function

$$a_0 \left[1 + a_1 \frac{\delta R_{\mu'_1}}{R_{\mu'_2}} \cos(p R_{\mu'_2}) \right]$$



Zhe Zhang et al. Phys. Rev. Lett. 112, 023204 (2014)

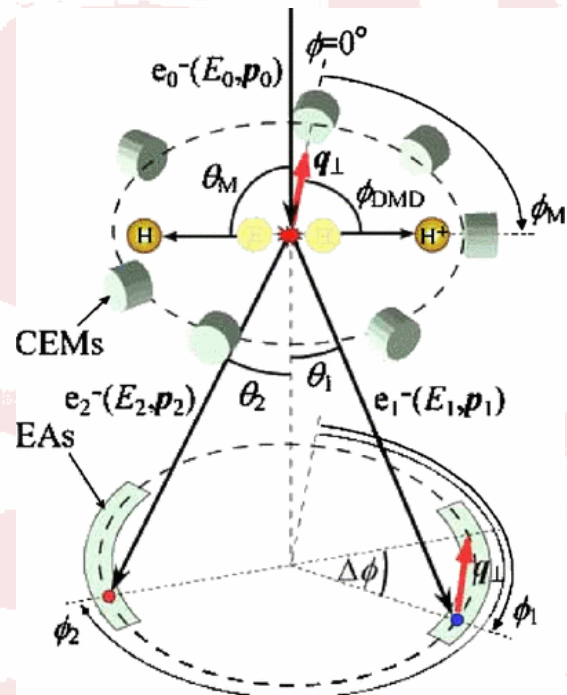
3. Molecular frame (e , $2e$) of H_2



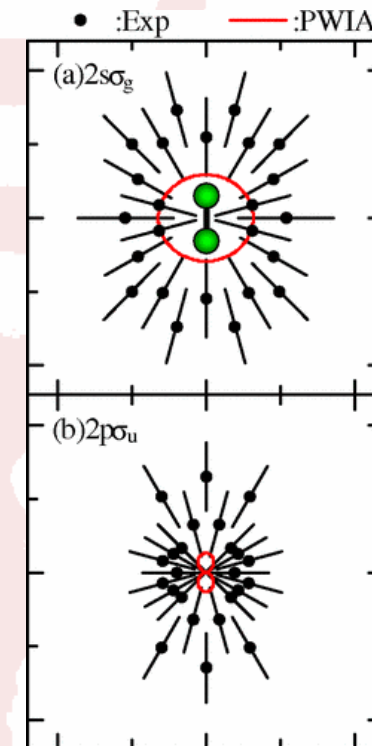
中国科学技术大学



axial-recoil approximation (to determine the molecular orientation)



(e , $2e+ion$)



Takahashi et al, Phys. Rev. Lett. 94, 213202

3. Molecular frame (e , $2e$) of H_2

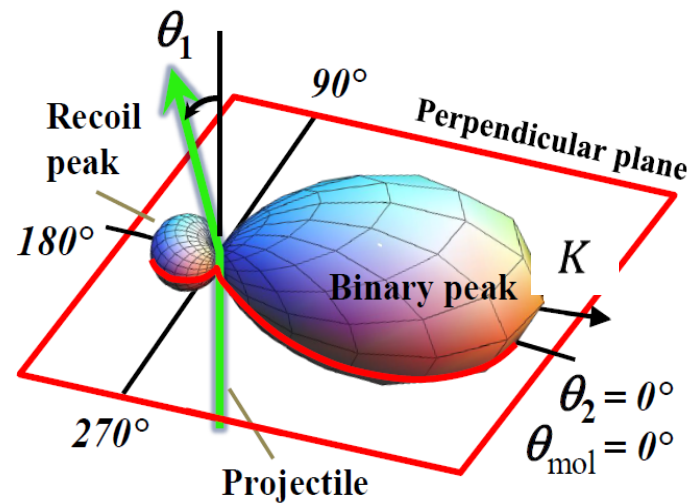
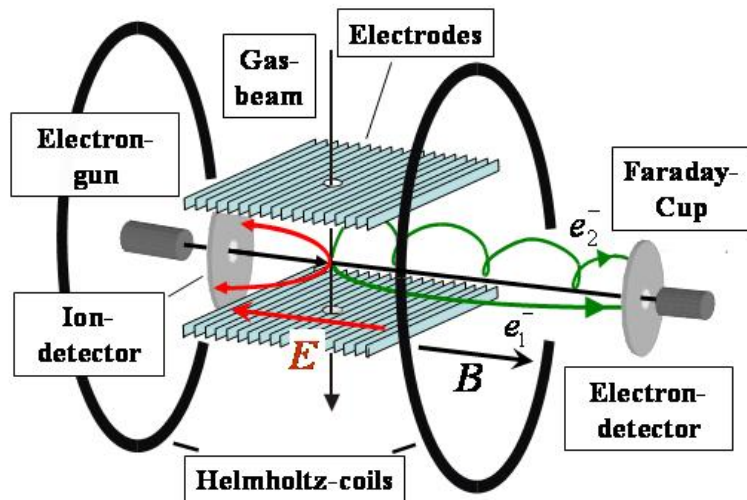


中国科学技术大学



Experiments:

Reaction Microscope



$$E_0 = 520 \text{ eV} \quad E_2 = 10 \text{ eV}$$

$$\theta_1 = 10^\circ, 20^\circ$$

the molecular axis is restricted to this perpendicular plane

3. Molecular frame (e , $2e$) of H_2



中国科学技术大学

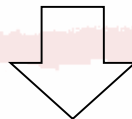


Theory:

Simple two-center interference model

Stia et al., Phys. Rev. A 66, 052709 (2002)

$$\sigma^{(6)} = \frac{d^6 \sigma_{H2}}{d\Omega_2 d\Omega_1 dE_1 d\Omega_R} = 2\sigma_H^{(3)} [1 + \cos(\chi \cdot R_e)]$$

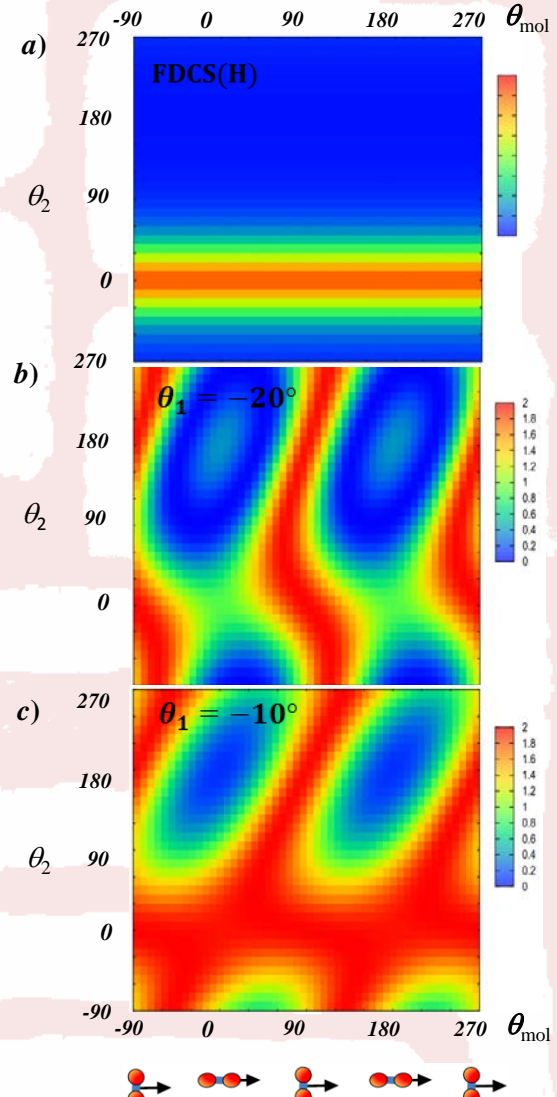


interference factor

$$\eta(\chi \cdot R_e) = \frac{\sigma^{(6)}}{2\sigma_H^{(3)}} = 1 + \cos(\chi \cdot R_e)$$

R_e is the internuclear vector

$$\chi = k_2 - K$$



3. Molecular frame (e, 2e) of H₂



中国科学技术大学



Multicenter distorted-wave (MCDW) method

$$\frac{d^6\sigma}{d\Omega_2 d\Omega_1 dE_1 d\alpha d\beta d\gamma}(\alpha, \beta, \gamma) = \frac{1}{(2\pi)^5} \frac{k_1 k_2}{k_0} |T_{fi}(\alpha, \beta, \gamma)|^2$$

$\Omega = (\alpha, \beta, \gamma)$ Euler angles

Transition amplitude:

$$T_{fi}(\Omega) = \left\langle \mathbf{k}_1 \Psi_f^{(-)}(\mathbf{k}_2; \mathcal{R}_{\Omega}^{-1}\{\mathbf{r}\}) \middle| V(\mathbf{r}) \middle| \mathbf{k}_0 \Psi_i(\mathcal{R}_{\Omega}^{-1}\{\mathbf{r}\}) \right\rangle,$$

Zhang et al, Phys. Rev. A 89 (2014) 052711

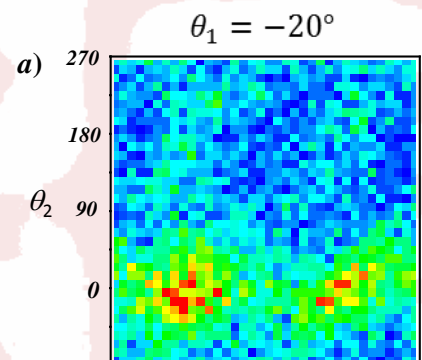
3. Molecular frame (e , $2e$) of H_2



中国科学技术大学



Experimental result

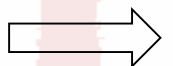


Xingyu Li et al, Phys. Rev. A 97 (2018) 022706

3. Molecular frame (e , $2e$) of H_2

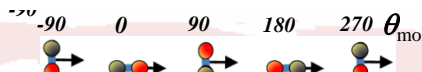
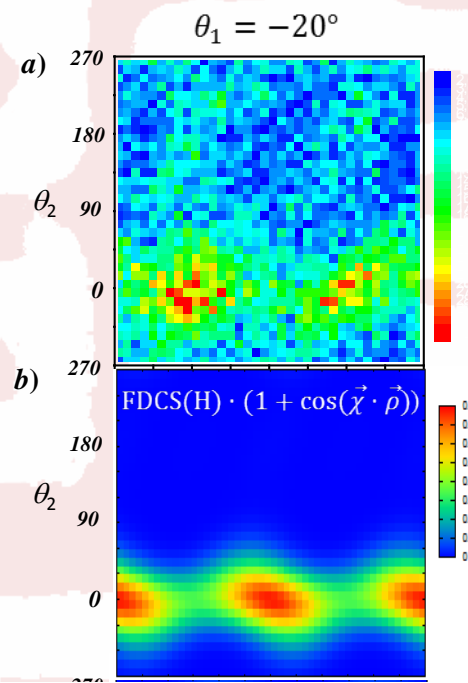
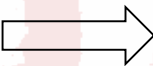


中国科学技术大学



Two-center interference model

$$\sigma^{(6)} = 2\sigma_H^{(3)} [1 + \cos(\chi \cdot R_e)]$$



3. Molecular frame (e , $2e$) of H_2



中国科学技术大学

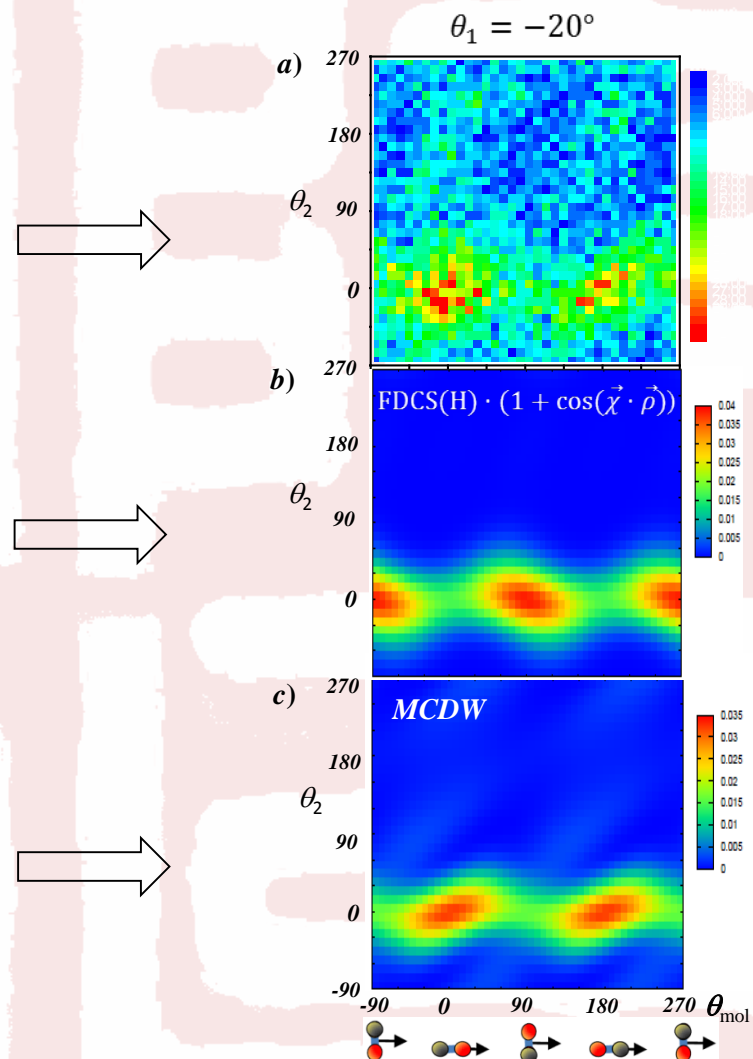


Experimental result

Two-center interference model

$$\sigma^{(6)} = 2\sigma_H^{(3)} [1 + \cos(\chi \cdot R_e)]$$

MCDW calculation



3. Molecular frame (e , $2e$) of H_2



中国科学技术大学

$$T \sim A_a e^{i\varphi_a} + A_b e^{i\varphi_b}$$

$$d\sigma^{(7)} \propto |T|^2 = A_a^2 + A_b^2 + 2A_a A_b \cos(\Delta)$$

